LATERAL WAVES

L. B. Felsen

Research Report No. PIBMRI-1303-65
Contract No. AF 19(628)-2357

Project No. 5635
Task No. 563501

for
AIR FORCE CAMBRIDGE RESEARCH LABORATORIES
OFFICE OF AEROSPACE RESEARCH
UNITED STATES AIR FORCE
BEDFORD, MASSACHUSETTS

15 November 1965

MRI

POLYTECHNIC INSTITUTE OF BROOKLYN
MICROWAVE RESEARCH INSTITUTE
ELECTROPHYSICS DEPARTMENT

NOTICES

Requests for additional copies by agencies of the Department of Defense, their contractors, or other government agencies should be directed to:

Defense Documentation Center (DDC)
Cameron Station
Alexandria, Virginia 22314

Department of Defense contractors must be established for DDC services or have their "need-to-know" certified by the cognizant military agency of their project or contract.

All other persons and organizations should apply to the:

Clearinghouse for Federal Scientific
and Technical Information (CFSTI)
Sills Building
5285 Port Royal Road
Springfield, Virginia 22151

AFCRL-65-889

LATERAL WAVES

L. B. Felsen

Polytechnic Institute of Brooklyn
Electrophysics Department
Graduate Center
Route 110
Farmingdale, New York 11735

Contract No. AF 19(628)-2357

Project No. 5635

Task No. 563501

Research Report No. PIBMRI-1303-65

15 November 1965

Prepared for

AIR FORCE CAMBRIDGE RESEARCH LABORATORIES
OFFICE OF AEROSPACE RESEARCH
UNITED STATES AIR FORCE
BEDFORD, MASSACHUSETTS

ACKNOWLEDGEMENT

The research reported in this report was sponsored by the Air Force Cambridge Research Laboratories, Office of Aerospace Research, under Contract No. AF 19(628)-2357.

ABSTRACT

When a radiator is located in a region wherein two or more wave types (1, 2..) may propagate with different speeds, and when a boundary coupling these wave types is present, diffraction phenomena may arise which are describable in terms of lateral waves. A lateral wave is launched by that portion of the incident field of type 1, for example, which gives rise to a field of type 2 refracted parallel to the boundary and which in turn refracts into a field of type 1. The most familiar example involves a plane interface separating two different semi-infinite dielectrics, and the associated wave types are the incident-reflected and the refracted waves. However, in anisotropic or in mechanically deformable media which may support several wave species, lateral waves are excited even in the absence of a second region.

The properties of lateral waves are reviewed in the transient and in the time-harmonic regimes. Concepts of wave coupling are emphasized, and general analytical features, as well as graphical procedures using refractive index diagrams, are described. Illustrative examples exhibit lateral waves on the interface between two homogeneous or inhomogeneous dielectrics, on a perfectly conducting plane immersed in an anisotropic and (or) compressible plasma, and also on a perfectly conducting half plane. The latter example shows how lateral waves may be diffracted by an edge discontinuity. Some relations between lateral waves, leaky waves, and spectral representations are also included.

TABLE OF CONTENTS

LIST OF ILLUSTRATIONS

LIST OF ILLUSTRATIONS (Contd)

I. Introduction

When a plane wave strikes a plane interface separating two different homogeneous, lossless, isotropic dielectrics, there arise reflected and refracted constituents in addition to the incident wave. If the field impinges from the denser medium (having the slower wave speed, and dielectric constant ϵ_1), the refracted wave emerges at a steeper angle with respect to the normal to the interface, and for incidence at the critical angle, refraction is parallel to the boundary. For still steeper directions of incidence, total reflection obtains and no propagating field is transmitted into the thinner medium (with dielectric constant ϵ_2). While the processes of reflection and refraction may generally be interpreted in simple ray-optical terms involving the concepts of wave fronts, rays, and ray tubes, this mechanism fails when incidence is along the critical angle. In this instance, the finite cross section of a tube of parallel incident rays shrinks to zero for the refracted rays parallel to the interface. The ray tube argument is directly relevant when excitation arises from a point source in the denser medium because the critically incident rays then lie on a single cone which may be surrounded unambiguously to form a corresponding ray tube. The rays bounding the tube after striking the interface belong to the reflected and also the refracted categories (see Fig. 1(a)), thereby making an interpretation difficult. It appears plausible that the critically refracted ray may react back on the denser medium by refraction (Fig. 1(b)), and since such a wave process cannot be explained by conventional geometrical optics, it must be a diffraction effect if it does indeed arise.

This paper is devoted to a review and further study of wave phenomena of this type, generally classed as "lateral waves", "head waves", or "refraction arrivals", with the latter terminology customary in the vocabulary pertaining to wave propagation in elastic media.[1] Each of these designations describes a special feature of the wave: the first highlights the lateral or sideways propagation of the wave parallel to the interface; the second derives from the fact that under transient conditions, this wave furnishes the first response in certain regions of the medium containing the source (see Fig. 6); and the third focuses on the important role played by refraction in

establishing the wave. In applications involving electromagnetics[2], the term "lateral wave" has found broad acceptance and will be retained here. The various characteristics of this wave on an ordinary dielectric interface are reviewed first for operation in either the transient or the time-harmonic regimes. Concepts of wave coupling involving the incident, reflected, and refracted constituents are emphasized, and refractive index diagrams[3] are employed to provide a graphical description of the wave front and ray trajectories, and also to clarify certain analytical features in the exact representation integrals for the fields from which the lateral wave may be extracted by rigorous techniques.* The interpretation in terms of wave coupling, and the use of refractive index diagrams, furnish additional insight which has been absent from the more conventional treatment.

Crucial for the existence of the lateral wave is the possibility of supporting wave propagation at two different speeds. In the example discussed, the different wave speeds occur in the denser and thinner medium, respectively, and the wave coupling at the interface produces a diffraction effect in the form of a lateral wave. If a single medium may support different wave speeds, lateral waves may arise at a bounding surface without the accessibility of a second region; in this instance, critical refraction and the associated wave coupling takes place among the various field types present. This aspect is illustrated for an anisotropic cold plasma wherein, for example, the ordinary and extraordinary waves have different propagation characteristics, and also for a warm plasma wherein one may find electronacoustic and ionacoustic waves in addition to those descriptive of electromagnetic phenomena. Depending on the number of wave types considered, it may be possible to have several kinds of lateral waves which arise from selective coupling between different species. An understanding of the coupling mechanism is furnished again by the refractive index diagrams (Figs. 7(b) and 11(a)).

---

*The lateral wave arises from a branch point contribution which must be accounted for during the asymptotic evaluation of the integral representation in the far zone (or at high frequencies). In the thinner medium, the lateral wave field is evanescent (see Fig. 1(b)).

The lateral wave constitutes a diffraction effect which is generally weaker than that associated with the direct and reflected (geometric optical) fields. This aspect does not constitute a handicap under transient conditions where different wave constituents at an observation point may be distinguished by their different arrival times; however, in the time-harmonic regime, the weakness of the response makes detection more difficult. An exception occurs when the direct and reflected fields are excluded from certain spatial regions which are nevertheless accessible to the lateral wave. This situation may arise when the denser of two media is inhomogeneous; the geometric-optical fields may then be confined to an illuminated domain, but excluded from the refraction shadow zone (Fig. 14(b)). The latter may, however, be penetrated by the lateral wave which then represents the dominant contribution. A similar situation may occur in a homogeneous, but anisotropic region with the confinement of the direct and reflected fields caused by the anisotropy (Fig. 7(a)). Losses in the denser region may serve to attenuate the conventionally dominant field constituents, thereby favoring the lateral wave, which propagates largely in the exterior low-loss medium (Fig. 15). These possibilities are illustrated by examples (Sec. V).

While the lateral wave progresses undisturbedly on a single infinite boundary, it is affected by other interfaces or by discontinuities. An example of the former is provided by a duct, formed either in the thinner or the denser medium. For the situation depicted in Fig. 2(a), interaction with the perfectly conducting plane takes place via the exponentially decaying lateral wave field in the thinner (fast speed) medium; evidently, the interaction is expected to be minimal when the duct width is large, but substantial for small ducts. Alternatively, when a duct exists in the slow-speed medium, the lateral wave should be influenced by multiple reflection (Fig. 2(b)). These anticipations are substantiated by analysis. The present examples also lend themselves to a discussion of the role played by the lateral waves in the spectrum of waves that can be guided along the interface. It is found that these strongly source-dependent waves do not belong to the proper mode spectrum but that they represent

the contribution from a portion of the continuous spectrum. In this regard, they resemble leaky waves, the connection with which is also explored (Sec. VII).

If the supporting surface is terminated abruptly, an impinging lateral wave may be scattered by the discontinuity generated in this manner. Two prototype problems are cited to demonstrate this effect; the boundary is a semi-infinite plane, embedded either in an anisotropic cold plasma or in an isotropic warm plasma. These problems show furthermore how lateral waves may be excited by structural discontinuities on the supporting surface (Sec. VI).

It is noted from Fig. 1(b) that the lateral wave exists only in a certain region of space bounded by the critically reflected ray (dashed line). In the vicinity of this ray boundary, the lateral wave field undergoes a rapid transition which cannot be described in simple ray-optical terms. A more complicated analysis is now required and is alluded to in the text (Sec. VIII). Analogous transition phenomena occur also for lateral wave species associated with configurations other than the simple dielectric in Fig. 1(b).

While the presentation here deals only with plane structures, it is to be expected that lateral waves may exist also on curved boundaries (Fig. 3). Although some preliminary studies of this more complicated phenomenon have appeared in the literature[4], further work is required to render an understanding of the behavior of this wave as complete as that of its simpler counterpart on a straight interface.

The preceding discussion has served to highlight salient physical aspects of lateral wave fields under rather general conditions. The further elaboration of these concepts, and some substantiation by analytical means, is to be found in the remainder of this paper. To simplify the analysis, the source configuration is taken to be a line distribution of electric or magnetic currents flowing parallel to the interface or boundary, thereby rendering the associated fields independent of the coordinate parallel to the source axis. No essential features are lost by this assumption; the choice of an arbitrarily oriented dipole source merely introduces azimuthal variation

and polarization effects which are not relevant to the present discussion, and also a distance decay characteristic of three-dimensional rather than two-dimensional propagation. Only the most familiar problem, involving a plane boundary separating two homogeneous isotropic dielectrics, is treated in some detail to provide an analytical foundation for the physical interpretation of the solution. The reliance in other examples is primarily on physical concepts, and no mathematical details are given in order not to extend further the length of this paper. The interested reader may wish to consult the source material referenced at appropriate places in the text.

II. Plane Boundary Separating Two Simple Homogeneous Regions

Lateral waves in their most familiar form arise when a spatially confined source configuration radiates from a homogeneous isotropic dielectric half-space which is separated by a plane interface from an optically thinner exterior region (Fig. 1(b)). Each half-space region is designated as "simple" since it supports wave processes at a single speed only. The solution and interpretation of the corresponding boundary value problem is reviewed in this section, both for the time-harmonic and for the transient regimes.

Also included here is the case where the medium containing the source is uniaxially anisotropic. While such a medium may in general support two wave speeds and is no longer "simple" in the sense defined above, only one wave type is required when the source distribution and the orientation of the anisotropy are chosen appropriately. The considerations in this section are confined to this special case and illustrate certain anomalous effects which are not encountered in an isotropic environment.

A. Two Isotropic Dielectrics

1. Time-harmonic regime

The boundary value problem for the configuration sketched in Fig. 1(b), with a line source parallel to the x-axis and located at $(y, z) = (0, z')$, is a classical

one in electromagnetic theory[2]. If the line distribution is composed of magnetic currents of unit strength, the magnetic field consists of the single component $H_x \equiv H$ from which the non-vanishing electric field components E_y, E_z may be derived by differentiation. The solution for H in the region $z < 0$ may be given in the form of a Fourier integral:[2,5]

$$H(y,z) = -\frac{\omega\epsilon_1}{\pm\pi}\int_{-\infty}^{\infty}\left[e^{i\varkappa_1|z-z'|} + \Gamma_\infty(\eta)e^{-i\varkappa_1(z+z')}\right]\frac{e^{i\eta y}}{\varkappa_1}\,d\eta \quad , \qquad (1)$$

where

$$\Gamma_\infty = \frac{\epsilon\varkappa_1 - \varkappa_2}{\epsilon\varkappa_1 + \varkappa_2} \quad , \quad \varkappa_j = \sqrt{k_j^2 - \eta^2} \quad , \quad \epsilon = \frac{\epsilon_2}{\epsilon_1} \quad , \quad k_j^2 = \omega^2\mu\epsilon_j \quad . \qquad (1a)$$

A time dependence $\exp(-i\omega t)$ is implied and suppressed. $\epsilon_{1,2}$ denote the dielectric constants in the two regions and μ is the permeability common to both. The imaginary part of the modal propagation constants $\varkappa_j$ is defined to be positive; for the lossless case ($\epsilon_{1,2}$ real), $\varkappa_j$ is positive when real. The integration path avoids the branch point singularities at $\eta = \pm k_{1,2}$ as shown in Fig. 4(a), and branch cuts are introduced to render the integrand single-valued on the four-sheeted Riemann surface. The pole singularity of Γ_∞ is not relevant to the present discussion.

The contribution from the first term inside the square bracket in (1) yields the field in the absence of the interface and may be represented in the closed form:

$$H_1(y,z) = -\frac{\omega\epsilon_1}{4}H_o^{(1)}(k_1 r) \quad , \qquad (2)$$

or asymptotically for large $k_1 r$,

$$H_1(y,z) \sim -\frac{\omega\epsilon_1}{4}\sqrt{\frac{2}{\pi k_1 r}}\,e^{i(k_1 r - \pi/4)}\left[1 + O\left(\frac{1}{k_1 r}\right)\right] \quad , \qquad (2a)$$

where r is the distance from the source to the observation point. No simple expression as in (2) is obtainable for the remaining integral H_2 which may, however,

be approximated by asymptotic techniques. If $k_1\hat{r} = k_1[y^2+(z+z')^2]^{1/2} >> 1$, where $\hat{r}$ is the distance from the source image to the observation point, the principal contribution to the integral arises from the vicinity of the saddle points in the integrand, and from any singularities which must be crossed during the deformation of the original integration path into the steepest descent path. The saddle points η_s are specified by the condition

$$\frac{d}{d\eta}[\varkappa_1|z+z'| + \eta y] = 0 \quad , \quad \text{or} \quad \frac{y}{|z+z'|} \equiv \tan\hat{\theta} = -\frac{d\varkappa_1}{d\eta} \text{ at } \eta_s \quad , \qquad (3)$$

which relation yields $\eta_s = k_1 \sin\hat{\theta}$, where $\hat{\theta}$ denotes the angle between $\hat{r}$ and the negative z-axis. Along the modified paths through the saddle point as shown in Fig. 4(b),* the integrand in H_2 is exponentially smaller than its value at η_s and the integral may therefore be approximated by its contribution arising from the vicinity of η_s. Since $|\eta_s| < k_1$ and $k_1 > k_2$, the branch point at $(+k_2)$ or $(-k_2)$ is intercepted when $k_2 < |\eta_s| < k_1$. The asymptotic approximation of H_2 thus contains the saddle point contribution,

$$H_2(y,z)\big|_{s.p.} \sim -\frac{\omega\epsilon_1}{4}\Gamma_\infty(\eta_s)\sqrt{\frac{2}{\pi k_1\hat{r}}}\, e^{i(k_1\hat{r}-\pi/4)}\left[1+O\left(\frac{1}{k_1\hat{r}}\right)\right] \quad , \quad k_1\hat{r} >> 1 \quad , \qquad (4)$$

and for $\sin\hat{\theta} > \sin\theta_c$, where $\theta_c = \sin^{-1}\sqrt{\epsilon_2/\epsilon_1}$ is the angle of critical refraction, also the branch cut integral contribution,

$$H_{2b}(y,z) \sim -\frac{\omega\epsilon_1}{\sqrt{2\pi}}\frac{\epsilon}{1-\epsilon}\frac{e^{i[k_1(L_1+L_3)+k_2L_2]+i\pi/4}}{(k_2L_2)^{3/2}}U(L_2) \quad , \quad k_2L_2 >> 1 \quad . \qquad (5)$$

The Heaviside function $U(L_2) = U(\hat{\theta}-\theta_c)$, which equals unity when its argument is positive and vanishes when its argument is negative, delimits the domain of existence of this field constituent. The saddle point yields the reflected wave of geometrical optics, while the branch point contributes a diffraction effect in the form of the lateral

---

*These paths follow the steepest descent contour in the vicinity of η_s only; they are sufficiently accurate for the present discussion and are much simpler than the complete steepest descent paths (see Fig. 19(b)).

wave (see Fig. 1(b) for a definition of $L_{1,2,3}$). The form of the phase function in (5) substantiates the interpretation in terms of a wave process which follows the trajectory in Fig. 1(b), and further support for this contention will be had from the transient analysis in Sec. 2.

While these elementary results are well-known[2,5], they are presented here to permit an interpretation via the refractive index diagram and also to emphasize the previously mentioned concept of wave coupling. The refractive index diagram is a plot of the directional dependence of the refractive index n, or equivalently, to within a constant factor, of the wave number $k = k_o n$ ($k_o = \omega\sqrt{\mu\epsilon_o}$ is the wavenumber in vacuum). The wave vector $\underline{k}$ appearing in a plane wave $\sim \exp(i\underline{k} \cdot \underline{r})$ specifies the direction of propagation of the phase front, and the corresponding normal to the refractive index diagram, the ray, specifies the direction of power flow (lossless conditions are assumed).[3] In the isotropic media considered above, the wave vector and ray are parallel since the refractive index diagrams are spheres with radii n_1 and n_2, respectively, as shown in Fig. 5. These plots represent equivalently $\varkappa(\eta) = k_o n_z(n_y)$ vs. $\eta = k_o n_y$; points on the curves yield propagating waves (real n_z), while the absence of a point n_z on the curve for a specified real value of n_y indicates a non-propagating solution (complex n_z). Evidently, propagating solutions in regions 1 and 2 occur only in the wavenumber intervals $|\eta| < k_o n_1 = k_o\sqrt{\epsilon_1/\epsilon_o} = k_1$ and $|\eta| < k_o n_2 = k_o\sqrt{\epsilon_2/\epsilon_o} = k_2$, respectively. Figure 5 shows where the double-valued functions $\varkappa_1(\eta)$ and $\varkappa_2(\eta)$ possess branch points. These singularities are located where two values of $\varkappa$ coalesce, and one observes that this happens at $\eta = \pm k_1$ and $\eta = \pm k_2$.

One notes from (3) that the saddle point η_s may be inferred from the wavenumber plot by a simple graphical construction: it corresponds to that point on the plot for region 1 for which the downward normal (i.e., the reflected ray) makes an angle $\hat{\theta}$ with the negative $\varkappa$-axis. The utility of the refractive index diagram in locating the saddle points of radiation integrals and in interpreting the resulting field contributions in ray-optical terms has been considered elsewhere in some generality and will

not be repeated here.[3] Instead, we proceed to a discussion of the lateral waves which are known to arise from branch point contributions. It has already been mentioned how the branch points may be located on the wavenumber diagram, and we shall now investigate the corresponding wave types. For the branch point at $\eta = k_2$, a ray (designated by 2) propagates parallel to the interface in the exterior medium 2, but the same value of η also admits of two propagating rays in medium 1: an upgoing ray 1 and a downgoing ray 3 inclined at the critical angle θ_c with the positive and negative z-axes, respectively (Fig. 5). These are precisely the ray trajectories in Fig. 1(b) which interpret correctly the asymptotic field contribution in (5). It is also evident from Fig. 5 that the resulting wave arises from the coupling of the two separate wave types in regions 1 and 2 at the boundary since both branches of the wavenumber diagram are involved. The diagram therefore permits the direct construction of the lateral ray trajectories and highlights the physical mechanism of the associated wave process. While the preceding remarks apply to the branch point at $\eta = k_2$, analogous considerations hold for $\eta = -k_2$ which gives rise to a lateral wave propagating in the opposite direction.

No such wave phenomena may be associated with the branch points at $\eta = \pm k_1$ since they do not admit of propagating waves in the second medium. This pair of branch points therefore does not give rise to lateral waves and, as noted from the analysis, it plays no special role in the asymptotic solution. It should also be noted that if the source is located in the optically thinner medium 2, one cannot construct a ray trajectory corresponding to that in Fig. 1(b) since there is no real incident ray which may excite a refracted ray parallel to the boundary. This follows at once from Fig. 5 because all directions of propagating incident rays in medium 2 are accomodated by the wavenumber interval $|\eta| < k_2$, and critical refraction in medium 1 does not occur in this range. A detailed analysis confirms the absence of a lateral wave in this instance.*

*It may be remarked that there exists a lateral wave in medium 1 which is excited by an evanescent incident wave from medium 2 and which refracts again into an evanescent wave. Because of the exponential damping associated with this field constituent in region 1, it is not considered further.

Upon comparing Eqs. (2), (4) and (5), it is observed that the lateral wave amplitude is $O(1/k_o L_2)$ with respect to that of the direct and reflected waves, at least at large lateral distances L_2 for which $r \approx \hat{r} \approx L_2$. Since $k_o L_2$ is a large quantity, the lateral wave field is dominated strongly by the geometric-optical field constituents and is therefore of secondary importance in problems of this type. An exception occurs when the source and observations points lie near the interface, in which instance the direct and reflected geometric optical waves cancel and the remaining $O(1/k_1 \hat{r})$ term in (4) becomes comparable to the lateral wave amplitude. A modification is required near the angle of total reflection where $L_2 \to 0$ in (5); the behavior in this transition region is described in Sec. VIII.

Finally, from an asymptotic evaluation of the fields in region 2 of Fig. 1(b), one finds[2] that there exists a geometric-optical constituent in the form of a refracted wave, and that the field corresponding to the lateral wave is evanescent. This is consistent with the ray diagram in Fig. 5 which does not provide for energy transfer from the lateral wave into medium 2. Such a transfer of energy is possible, however, under more general conditions where medium 2 may support two or more distinct wave speeds; in this instance, the lateral wave sheds propagating rays into both regions. This aspect is explored further in Sec. IV.

2. Transient regime

While the time-harmonic lateral wave field in the preceding configuration constitutes a second order effect as compared to other field constituents, this is not true under transient conditions as will now be demonstrated. Although the response to excitation by a pulsed source may be evaluated for arbitrary observation times[6,7], it suffices for the purposes of the present discussion to consider initial field values only. These may be recovered from the time-harmonic high-frequency solutions in (2a), (4) and (5) by recourse to well-known asymptotic properties of the Laplace transform. Namely, if $\hat{u}(\underline{r}, t)$ denotes a function of space and time which

vanishes identically when $t < t_o$, and if $u(\underline{r}, s)$ is its temporal Laplace transform,

$$u(\underline{r}, s) = \int_{t_o}^{\infty} e^{-st}\hat{u}(\underline{r}, t)dt = e^{-st_o}\int_{o}^{\infty} e^{-s\xi}\hat{u}(\underline{r}, \xi+t_o)d\xi \quad , \tag{6}$$

where (Re s) is positive and large enough to assure convergence of the integral, then the principal contribution to the integral for large s arises from the vicinity of $\xi = 0$. Let us assume that $\hat{u}(\underline{r}, t)$ behaves near $t = t_o$ according to

$$\hat{u}(\underline{r}, t) \sim \xi^{\alpha}(d_o + d_1\xi + d_2\xi^2 + \ldots) \quad , \quad \text{Re } \alpha > -1 \quad , \quad \xi = t - t_o \quad , \tag{7}$$

where the d_n depend on $\underline{r}$ only. Then by substituting (7) into (6), inverting the orders of summation and integration, and utilizing a well-known integral formula for the gamma function $\Gamma(x)$, one obtains the asymptotic expansion of $u(\underline{r}, s)$ for large s,

$$u(\underline{r}, s)e^{st_o} \sim \sum_{n=0}^{\infty} \frac{d_n}{s^{\alpha+n+1}}\Gamma(\alpha+n+1) \quad . \tag{8}$$

*

When s in (8) is replaced by $(-i\omega)$, this result describes the high-frequency behavior of the time-harmonic field $u(\underline{r}, -i\omega)$. Since the same coefficients d_n appear in (7) and (8), the transient response near the time of arrival $t = t_o$ of the first signal may be deduced from the time-harmonic high-frequency result, and vice versa. If the right-hand side of (8) also contains multiplicative integral powers of s, these may be interpreted as time derivatives of the transient field.

These considerations may now be applied to the formulas in (2a), (4), and (5). Upon writing (2a) in the form

$$H_1(y, z) \sim i\omega \left\{ \frac{\epsilon_1}{2\sqrt{2}\ \pi\sqrt{r/c_1}} \frac{e^{i\omega\, r/c_1}}{(-i\omega)^{1/2}} \Gamma(\tfrac{1}{2}) \right\} \quad , \tag{9}$$

---

*The gamma function in this section is not to be confused with the reflection coefficient denoted elsewhere by the same symbol.

where $c_1 = (\omega/k_1)$ is the propagation speed in medium 1* and it has been recognized that $\Gamma(1/2) = \pi^{1/2}$, one finds by comparison with (7) and (8) the following transient solution,

$$\hat{H}_1(y, z;t) \sim -\frac{\partial}{\partial t}\left\{\frac{\epsilon_1}{2\sqrt{2}\,\pi\sqrt{r/c_1}}\,\frac{1}{[t-(r/c_1)]^{1/2}}\right\} \quad , \quad t \approx \frac{r}{c_1} \quad . \tag{10}$$

The excitation for this time-dependent field is the temporal impulse $\delta(t)$ whose Laplace transform equals unity and therefore does not appear explicitly in (9). This conclusion may also be verified from the known exact solution for the impulsive line source field[7],

$$\hat{H}_1(y, z;t) = -\frac{\partial}{\partial t}\left\{\frac{\epsilon_1}{2\pi}\,\frac{1}{[t^2-(r/c_1)^2]^{1/2}}\right\} \quad , \quad t > \frac{r}{c_1} \quad , \tag{11}$$

which reduces to (10) when $t \approx (r/c_1)$. It is understood in (10) and (11) that $\hat{H}_1 \equiv 0$ when $t < \frac{r}{c_1}$. Evidently, the primary field is in the form of a cylindrically spreading disturbance which originates at the source at time $t = 0$ and reaches the observation point after the time interval $t = (r/c_1)$ required for the signal to traverse the distance r at the propagation speed c_1.

In a directly analogous manner, the reflected field in (4) corresponds to a temporal response

$$\hat{H}_2(y, z;t)\big|_{s.p.} \sim -\frac{\partial}{\partial t}\left\{\frac{\epsilon_1}{2\sqrt{2}\,\pi\sqrt{\hat{r}/c_1}}\,\frac{\epsilon\cos\hat{\theta}-\sqrt{\epsilon-\sin^2\hat{\theta}}}{\epsilon\cos\hat{\theta}+\sqrt{\epsilon-\sin^2\hat{\theta}}}\,\frac{1}{[t-\frac{\hat{r}}{c_1}]^{1/2}}\right\} \quad , \quad t \approx \frac{\hat{r}}{c_1} \quad , \tag{12}$$

which represents a cylindrically spreading disturbance that appears to emanate from the image point and arrives at (y, z) after a time interval $t = \hat{r}/c_1$. Since $\hat{r} > r$, the reflected pulse is received after the primary signal.

---

*The dielectrics are assumed to be dispersionless so that $\epsilon_{1,2}$ are constants independent of frequency.

Finally, upon writing the lateral wave contribution (5) in the form

$$H_{2b}(y,z) \sim i\omega \left\{ \frac{\sqrt{2}}{\pi} \frac{\epsilon_2}{(1-\epsilon)(L_2/c_2)^{3/2}} \frac{e^{i\omega[\frac{L_1+L_3}{c_1}+\frac{L_2}{c_2}]}}{(-i\omega)^{3/2}} \Gamma(\tfrac{3}{2}) \right\} U(L_2) \quad , \tag{13}$$

one derives the transient solution for $t \approx T \equiv (L_1+L_3)/c_1+(L_2/c_2)$,

$$\hat{H}_{2b}(y,z;t) \sim -\frac{\partial}{\partial t} \left\{ \frac{\sqrt{2}}{\pi} \frac{\epsilon_2}{(1-\epsilon)(L_2/c_2)^{3/2}} [t-T]^{1/2} \right\} U(L_2) \quad , \tag{14}$$

with the understanding that the first response arrives at time $t = T$. Unlike the direct and reflected fields which spread cylindrically, the lateral wave front is planar and may reach certain observation points before any other signal. This feature, arising from the fact that a portion of the wave propagates in the second medium with speed $c_2 > c_1$, accounts for the previously mentioned designation of "head wave" and serves to clearly distinguish the lateral wave response from the remaining constituents. This is true despite the fact that the field discontinuities across the impinging lateral wave front are weaker than those associated with the direct or reflected signals (see (10), (12), and (14)). Thus, in contrast to the time-harmonic case, the transient lateral wave response is not obscured by the stronger direct and reflected fields.

The configuration of wave fronts associated with the various field constituents is shown in Fig. 6 for the special case where the source lies in the interface. This implies that $r = \hat{r}$ and $L_1 = 0$, thereby simplifying the drawing. The direct and reflected fronts now coalesce along the semi-cylindrical surface $r = c_1 t$ (Fig. 6(a)), while the lateral wave front in the region $\hat{\theta} > \theta_c$ is given by $[L_3 + L_2 \sin\theta_c] = c_1 t$, where $\sin\theta_c = (c_1/c_2)$ is the critical angle (Fig. 6(b)). Also shown (Fig. 6(c)) is the refracted wave front which spreads cylindrically into the upper medium with speed c_2. When these fronts are combined into the single picture in Fig. 6(d), one observes that observation points in the vertically shaded region are reached first by the lateral wave. Fig. 6(d) also illustrates why a lateral wave constituent must be present. The direct signals in regions 1 and 2 propagate

with speeds c_1 and c_2, respectively, and since $c_2 > c_1$, the field from the high-speed region spills over into the low-speed region to provide for the required continuity across the interface. This spill-over effect gives rise to the lateral wave. It is readily verified that points along the lateral wave front are reached by ray trajectories L_2 and L_3 as sketched in Fig. 1(b), thereby confirming the validity of the ray diagram.

This concludes the discussion of the role played by the lateral wave in the well-explored configuration involving two homogeneous, isotropic dielectrics. The purpose of this review has been to establish and substantiate relevant concepts on a familiar example. In subsequent problems wherein the medium characteristics are more general, recourse will be had to the physical concepts emphasized above, without detailed mathematical justification. The reader interested in the analytical treatment may wish to look up the references which are cited at appropriate places in the discussion.

B. Isotropic and Uniaxially Anisotropic Dielectrics

1. Line source excitation

In an anisotropic dielectric, the propagation characteristics depend on direction so that the refractive index plot is no longer spherical. While there exist in general two distinct wave species, customarily called "ordinary" and "extraordinary", it is possible to select special source distributions which excite only one of these wave types. The simplest example which nevertheless retains distinctive features of anisotropy involves a uniaxially anisotropic medium excited by a magnetic line current oriented perpendicular to the optic axis. The medium is characterized by the dielectric tensor $\underset{\sim}{\epsilon} = (\underline{u}_o\underline{u}_o + \underline{v}_o\underline{v}_o)\epsilon_1 + \underline{w}_o\underline{w}_o\epsilon_2$, where $\underline{u}_o$, $\underline{v}_o$ and $\underline{w}_o$ are unit vectors parallel to the u, v, and w axes, respectively. A cold plasma under the influence of a strong external magnetic field along the w-axis exhibits uniaxially anisotropic properties of this type, with $\epsilon_1 = \epsilon_o$ and $\epsilon_2 = \epsilon_o(1-\omega_p^2/\omega^2)$, where ϵ_o is the dielectric constant of vacuum while ω_p and ω represent the plasma

and applied frequencies, respectively. It may readily be shown[8] that the corresponding refractive index surface has two branches, one of which is spherical while the other is either spheroidal or hyperboloidal depending on whether $\epsilon_2 > 0$ or $\epsilon_2 < 0$, respectively, with $\epsilon_1 > 0$. When the fields are generated by a magnetic line source parallel to the x-axis, only the last described wave species is excited and suffices for a complete description even in the presence of a plane interface which separates the anisotropic medium from an isotropic one. This configuration is shown in Fig. 7(a), and the composite wavenumber plot (for $\omega < \omega_p$) is given in Fig. 7(b)).

An analysis of the problem leads to an integral representation for the magnetic field $H_x \equiv H$ which is similar to that in (1) except that $\kappa_1(\eta)$ now has a form descriptive of the hyperbolic shape of the wavenumber surface[8]. A study of Fig. 7(b) reveals the existence of only one set of branch points on the real η-axis, namely at $\eta = \pm k_o$. From an asymptotic evaluation, one deduces three contributions to the field in the plasma region: the direct and reflected waves which arise from saddle points, and the lateral waves which arise from branch points. These field constituents may be interpreted in terms of ray optics; salient features of the field deduced directly from the refractive index plot are found to be in complete agreement with the analytical results.[8] In particular, since the refractive index diagram for the plasma medium has an open branch, the direct and reflected rays are confined to certain angular regions in space, thereby creating a shadow zone as shown in Fig. 7(a). The dashed lines emanating at the source define the limiting incident rays, and the second set of dashed lines represents the limiting reflected rays; since neither the direct nor the reflected rays penetrate beyond these lines, they constitute the shadow boundary.

The lateral wave which follows the trajectory in Fig. 7(a) is not excluded from the geometrical shadow region. Its variation may be shown to be as follows:[8]

$$H_{2b} \propto \frac{e^{ik_o[L_1 N(\theta_1) + L_3 N(\theta_3) + L_2]}}{(L_2)^{3/2}} U(L_2) \quad , \tag{15}$$

an expression similar to that in (5) except that the ordinary refractive index n is replaced by the ray refractive index $N(\theta)$ which depends on the angle θ between the ray and the positive z-axis. ($N = n \cos \alpha$, where α is the angle between the ray and $\underline{k}$). $L_{1,2,3}$ are the ray paths predicted from the refractive index plot. In a similar manner, one may use the plot to construct a lateral wave solution propagating to the left.

An important feature is contained in this result for a half space region comprised of even such a simple anisotropic medium as the uniaxial: the lateral wave field is dominant in the shadow zone which is not penetrated by the direct or reflected field constituents. Thus, under appropriate conditions of excitation, there may exist in a homogeneous anisotropic half-space certain spatial domains wherein the lateral wave does not compete with stronger contributions to the field but is itself the dominant constituent. This aspect, which does not arise in the analogous isotropic environment, lends further significance to the lateral wave field.

2. Excitation by a highly directive source

An interesting "thought experiment" may be performed to lend further support to the validity of the trajectory sketched in Fig. 7(a). From the discussion in Sec. I, it is recalled that critical refraction plays an essential role in the explanation of the wave processes associated with the lateral wave contribution. It may then be expected that the lateral wave is strongly excited by a source configuration which emits substantial radiation along the critical angle, but that small amplitudes result when this condition is not satisfied. A highly directive source whose radiation pattern is given by a narrow beam is suited to this purpose. Such a source may be realized by a linearly phased current distribution which extends over many wavelengths and whose beam may be scanned by altering the phase constant. The far-zone fields of this antenna in the presence of an anisotropic half space are easily calculated and yield essentially the line source result multiplied by an "array factor".[9] The array factor associated with the lateral wave is found to be small unless the incident beam (i.e., the incident ray representative of the power carried

in the beam) points along the critical direction; in the latter instance, the array factor, and therefore the lateral wave field amplitude, shows a strong peak (Fig. 8).[9] This phenomenon is particularly striking in the shadow region of Fig. 7(a) wherein the lateral wave yields the only significant contribution, and it confirms the essential role played by critical refraction in the establishment of the lateral wave.

III. Bounded Region Supporting Several Wave Species

The preceding examples have illustrated the propagation characteristics of lateral waves in the most familiar situation comprising two homogeneous half spaces, each capable of supporting only a single wave species (this is true for ordinary dielectrics and also for the special case of the aforementioned uniaxially anisotropic medium). The previously emphasized wave coupling plays an important part in explaining the propagation mechanism and evidently involves fields which are associated with two distinct spatial regions. In media of more general makeup which may individually support two or more wave species, this coupling arises between different wave types along a boundary in the same medium but is otherwise directly analogous to the situation in Sec. II. Several specific examples will now be discussed, and the conclusions are then extrapolated to regions exhibiting propagation characteristics of extreme generality.

A. Isotropic Warm Plasma

A simple and timely example of an isotropic medium capable of supporting wave processes at different speeds is provided by a plasma formed of a collection of electrons, ions, and neutral particles. To a lowest order of approximation, the effect of this medium on an electromagnetic wave may be represented by an equivalent dielectric constant of the form $\epsilon = \epsilon_o [1 - (\omega_p^2/\omega^2)]$, where ω_p and ω denote the plasma frequency (for electrons) and the wave frequency, respectively.[10a] In this simplest model, the ions provide a stationary neutral background, and the electrons oscillate about their stationary equilibrium position due to the influence of

the (weak) impinging electromagnetic field. If the thermal motion of the electrons is taken into account, one is led to the definition of a dynamical pressure p descriptive of acoustic effects in the electron gas, and the resulting medium may now support two wave species:[10b] an electromagnetic (also frequently called an "optical") wave which contains all of the magnetic field and has no charge accumulation, and a dynamical (often referred to as "electronacoustic") wave which has all of the charge accumulation but no magnetic field. The two wave processes exist independently in an unbounded homogeneous plasma and proceed at different speeds: the electromagnetic wave is characterized by a wavenumber $k = k_o\sqrt{\epsilon} = (\omega/c)\sqrt{\epsilon}$ where ϵ is the previously defined dielectric constant of the cold (incompressible) plasma, while the electronacoustic wave is characterized by a wavenumber $k_a = k(c/a) = (\omega/a)\sqrt{\epsilon}$, where c is the electromagnetic propagation speed in vacuum and "a" is the acoustic propagation speed in the electron gas. When a boundary is interposed along which the impinging electromagnetic wave has a perpendicular electric field component, wave coupling must be introduced in order to satisfy the boundary conditions on the composite electromagnetic and dynamical fields.[11]

The simplest configuration involves a homogeneous compressible plasma which exists in a half space region bounded by a perfect conductor. The wavenumber or refractive index plot for the medium consists of two concentric spheres as in Fig. 5 since the wave processes are isotropic; however, the radii are now given by k and k_a for the electromagnetic and acoustic waves, respectively (Fig. 9). One observes from the diagram that a lateral wave is excited by an incident electron acoustic ray 1* which refracts into ray 2 propagating with the electromagnetic speed parallel to the boundary and which sheds energy back into the electronacoustic field along ray 3. It is also noted from the diagram that the reverse process cannot exist;

---

*A line distribution of electric dipoles oriented perpendicularly to the line axis is a suitable source; a magnetic line current does not excite an incident dynamical wave.

i.e., there is no lateral wave excited by an incident electromagnetic field since one cannot find a corresponding electronacoustic ray path parallel to the boundary. From these trajectories, one constructs the phase characteristics of the lateral wave as follows:

$$p_b \propto \frac{e^{i[k_a(L_1+L_3)+kL_2]}}{(L_2)^{3/2}} U(L_2) \quad , \tag{16}$$

where p denotes the electronacoustic pressure, and the restricted domain of existence of the wave as expressed by the step function $U(L_2)$ follows from Fig. 9(b). The amplitude dependence on distance $\sim (L_2)^{-3/2}$ is not predictable from the wavenumber plot, but may be anticipated from the result in (5); this variation is typical of the branch cut integral contribution (subscript b in (16)) in the rigorous analysis which yields the lateral wave constituent. It may be remarked that these simple considerations are substantiated completely by a rigorous solution of the boundary value problem[12] which, of course, yields as well additional space-independent factors entering into the amplitude function.

Attention should be called to the complete analogy of the ray trajectories sketched in Fig. 9(b) with those for the two-medium problem in Fig. 1(b), provided that all wave processes are now taken to occur in the same medium. The analogy can be carried even further to the construction of the wave fronts; the resulting picture is shown in Fig. 9(c) and is obtained by folding the upper portion of the drawing in Fig. 6(d) onto the lower portion.* While wave phenomena of the type sketched in Fig. 9 are novel in electromagnetics, they are familiar in the theory of wave propagation in elastic media.[1b]

B. Uniaxially Anisotropic, Cold Plasma

A somewhat more complicated example of a configuration capable of supporting wave processes at different speeds is provided by an anisotropic medium. Even in the simplest case of uniaxial anisotropy, there exist two distinct wave species,

*This simple picture applies only when the wave processes are non-dispersive and should therefore not be taken literally for the warm plasma.

the ordinary and extraordinary. While only one of these is excited by the source arrangement described in Sec. IIB1, both wave types must be considered in a more general situation. This is found to occur, for example, when a line of magnetic currents is inclined at an arbitrary angle $\bar{\theta}$ with respect to the optic axis as shown in Fig. 10(a), in which instance both the ordinary ("o") and extraordinary ("e") waves are excited by the source and are coupled at the perfectly conducting boundary.[13] Since the fields are independent of the x-coordinate and the line direction and optic axis are assumed to be contained in the x-z plane, the relevant portion of the refractive index diagram is the intersection of the surface of revolution in the ξ-η-$\varkappa$ wavenumber space (Fig. 10(b)) with the plane $\xi = 0$ (ξ is the wavenumber in the x-direction)(Fig. 10(c)).*

The existence of a lateral wave may again be predicted by studying the ray configurations obtained from the wavenumber plot. In reference to Fig. 10(c), it must be kept in mind that rays 1 and 3 are projections on the y-z plane only since the actual rays drawn normal to the wavenumber surface in Fig. 10(b) in the $\xi = 0$ plane possess as well a component along the ξ(or x) axis. Thus, the true lateral wave trajectory is not the one shown in Fig. 10(d) but it possesses as well a displacement parallel to x. One observes that the lateral wave is excited by an incident "e" ray 1 which couples to a critically refracted "o" ray 2 traveling along the boundary; this ray then refracts into "e" ray 3. The analytical form of the lateral wave contribution is then constructed as before and leads to an expression as in (15) except that $L_{1,2,3}$ now refer to the ray paths in the present problem. Only one lateral wave, existing to the right of the dashed line, has been shown in Fig. 10(d); a similar wave exists in the left-hand region and its trajectory and coupling mechanism may be determined by analogous considerations. All of these conclusions have been confirmed by rigorous

*In the example of Sec. IIB1, the line source (along x) is oriented perpendicularly to the optic axis which lies in the y-z plane. The $\xi = 0$ plane then intersects the wavenumber surface in the trace shown in Fig. 7(b), and all of the normals to the surface are contained in the $\xi = 0$ plane.

analysis.[13]

C. Arbitrary Medium

From the preceding graphical considerations which have been confirmed by rigorous solutions of special problems, one may predict the occurrence and the type of lateral waves which arise under quite general conditions. It shall be assumed that the medium in question can support several wave types, each of which possesses a known refractive index surface. An example is provided by a multi-species (electrons and ions) compressible plasma under the influence of an external d.c. magnetic field, which is characterized by a variety of wave solutions with different propagation characteristics. Consider, for example, a multi-branched wavenumber surface whose relevant portion (for line source excitation along the x-axis) is the section shown in Fig. 11(a). Along a perfectly conducting boundary at $z = 0$, wave coupling occurs which gives rise to a multiplicity of lateral waves. As previously, the existence of such waves is predicted by the ability to draw a ray trajectory which contains an incident ray, a ray refracted parallel to the boundary in another wave species, and still another refracted ray which carries energy back into the medium. One observes from Fig. 11(a) that three such possibilities exist.* The simplest corresponds to coupling between wave types 3 and 4, with the former providing the lateral portion while the latter accounts for the incident and emerging fields. The resulting trajectory, quite similar to the one in Fig. 10(d), is shown in Fig. 11(b_1). Somewhat more complicated is the lateral wave which couples wave types 2, 3, and 4, with 2 representing the lateral portion and either 3 or 4 furnishing the incident or emerging rays. In this instance, the wave can be excited by incident rays of either type 3 or 4, and energy leakage takes place into either types 3 or 4. Possible ray paths are now: 4′-2′-4′, 4′-2′-3′, 3′-2′-4′, 3′-2′-3′, which express the various combinations (Fig. 11(b_2)). Still more diversified is the wave for which species 1 provides the lateral portion (Fig. 11(b_3)). In all cases, the lateral wave field varies

*As noted earlier, the points corresponding to lateral rays 1, 2′, 3″ on the refractive index diagram also yield the real contributing branch points of the multi-valued function $\kappa(\eta)$.

according to (see also (15))[14]

$$A \frac{e^{ik_o[L_iN_i(\theta_i)+L_jN_j(\theta_j)+L_kN_k(\pi/2)]}}{L_k^{3/2}} U(L_k) \quad , \tag{17}$$

where L_i, L_j and L_k represent the path lengths along the incident, emerging, and lateral portions of the trajectory, respectively, while θ_α and $N_\alpha(\theta_\alpha)$ denote the corresponding ray angles (measured from the normal to the interface) and ray refractive indeces. A is a factor which depends on the source strength, on the medium parameters and on k_o but not on the space variables $L_{i,j,k}$.

A remark is in order on how these ray trajectories are employed in an actual calculation of the field at an observation point P. Consider, for example, the three lateral waves excited by incident ray 2 (last diagram in Fig. 11(b_3)). One constructs the refracted rays 2, 3, 4 in such a manner that they arrive at P along the direction required from the refractive index plot. The intersection of these rays with the interface then determines the lateral segments $L_1^{(2)}$, $L_1^{(3)}$, and $L_1^{(4)}$, respectively, as shown in Fig. 11(c). It must be kept in mind that Fig. 11 has only the projection of the trajectory on the y-z plane, and that there may in general be displacements parallel to x although the source and observation points lie in the y-z plane (thus, the lateral segments for the three waves need not be colinear). The total field at P is the sum of all possible wave solutions which may propagate from the source to P along trajectories consistent with the refractive index diagram.

IV. Plane Boundary Separating Two Homogeneous, But Otherwise Arbitrary Media

We are now ready to proceed to the most general situation wherein two arbitrary, but homogeneous, media are separated by a plane interface, and a source is embedded in one of the half-space regions. By invoking the frequently emphasized viewpoint of wave coupling at the boundary, this problem differs only slightly from the one discussed in Sec. IIIC wherein only one region is accessible. In the present instance, one merely examines the refractive index surfaces for the <u>composite</u> region

and deduces the lateral wave trajectories accordingly. For example, let us assume that the surfaces labeled 1 and 2 in Fig. 11(a) describe propagation in the upper region $z > 0$, while the remaining surfaces 3 and 4 characterize propagation in the lower region $z < 0$ (if surfaces 1 and 2 are spheres, they might be descriptive of an isotropic compressible plasma occupying the upper half space (see Fig. 9(a)), while surfaces 3 and 4 are representative of the ordinary and extraordinary waves, respectively, in a cold anisotropic plasma filling the lower half space). The refractive index plot for the composite region is then precisely the one in Fig. 11(a), and the determination of the lateral wave fields proceeds as before. If the source is in the lower region, a lateral wave may be excited which follows the same trajectory as in Fig. $11(b_1)$. Fig. $11(b_2)$ is also applicable provided that the lateral segment $2'$ is drawn in the upper region since only the upper medium supports wave type 2 (see Fig. 12(a)). Neither the 3-4 nor the 2-3-4 coupling mechanism leads to an energy transfer into the upper half space. However, the lateral wave which arises from the coupling of all the wave species 1-2-3-4 sheds energy both into the upper and lower regions as shown in Fig. 12(b). The analogue of the third sketch in Fig. $11(b_3)$ is not relevant since no incident ray 2 is available from the lower medium; such a possibility does exist, however, when the source is located in the upper half space.

The analytical dependence of the field is the same as in (17),[15] and it should now be clear how certain salient features of the lateral waves under quite general conditions may be predicted directly from the refractive index plots.*

V. Configurations Wherein the Lateral Wave Field is Dominant

While the preceding discussion has dealt only with the lateral wave contribution to the far field of a confined source distribution, it must be kept in mind that there exists in addition a geometric-optical (direct and reflected or refracted) field

---

*For information concerning polarization effects and the factor A in (17), a more detailed analysis is required.[14]

which generally predominates over the lateral wave because of the latter's more rapid decay with lateral distance (see (2), (4) and (5)). Although this aspect is not detrimental in the transient regime where the various field constituents at an observation point may be distinguished by their different arrival times (see Sec. IIA2), it poses a problem under time-harmonic conditions. It is therefore relevant to explore time-harmonic situations wherein the lateral wave contribution is the only important one and is therefore easily detectable. This requires, in essence, an arrangement which eliminates the geometric-optical field without affecting the lateral wave.

A. Homogeneous, Anisotropic Medium

One such arrangement has already been explored in a special example (Sec. IIB), and relies on certain types of anisotropy to confine the direct and reflected rays to certain limited regions of space. This happens when the refractive index plot has an open branch because the range of propagating wave solutions is then restricted to a certain angular region about the gyrotropic axis. When a boundary or interface is interposed, the reflected rays are similarly confined, but no such limitation applies to the lateral wave which freely penetrates the geometric-optical shadow region (Fig. 7(a)) and represents the dominant field contribution there.

B. Inhomogeneous Medium

The confinement of the geometric-optical field to certain limited regions of space may also be brought about by inhomogeneities even when the medium is isotropic. An example is provided by a continuously stratified dielectric having a profile as shown in Fig. 13(a); such a variation is characteristic of a plasma medium whose electron density increases from zero at $z = \infty$ monotonically toward the origin. When a line source is placed into the region at an elevation $z' > z_1$ and the frequency is high enough to justify the application of ray optics, the rays emanating at the source are refracted by the medium inhomogeneity into a zone of illumination which is separated from the remaining shadow zone by the envelope (caustic) of the refracted

ray system (Fig. 13(b)).[16]

If the inhomogeneous medium is separated by a plane interface at $z = z_o$ from a homogeneous half space with dielectric constant $\epsilon_1 < \epsilon(z_o)$ (see Fig. 14(a)), one obtains the ray configuration in Fig. 14(b) which comprises reflected rays and rays refracted into the lower region, in addition to those sketched in Fig. 13(b). This complex of rays is still confined to a limited region of space which is bounded by the previously described caustic, except near the interface where it is bounded by the glancing ray. A lateral ray is launched by that incident ray which arrives at the interface at the critical angle; the resulting trajectory 1-2-3 in Fig. 14(b) shows that the refracted ray 3 penetrates the geometric-optical shadow region where it constitutes the dominant contribution to the field. The lateral wave behavior is now given by:

$$\frac{A\, e^{ik_o\left[\int_{L_1} n(z)\underline{s}_1 \cdot d\underline{r} + \int_{L_3} n(z)\underline{s}_3 \cdot d\underline{r} + L_2 n_1\right]}}{L_2^{3/2}} U(L_2) \quad , \tag{18}$$

where L_1, L_2 and L_3 denote the path lengths along rays 1, 2, and 3, respectively, $\underline{s}_{1,3}$ are unit vectors tangent to rays 1 and 3, and $n = \sqrt{\epsilon/\epsilon_o}$ is the refractive index.

Evidently, a combination of the effects described in this section and the preceding one may be anticipated when the medium is inhomogeneous and anisotropic.

C. Lossy Medium

A third, and quite simple, mechanism for removing the geometric-optical field at large lateral distances is the presence of dissipation which is effective in all of the cases discussed so far. Let the half-space containing the source be lossy, but let the exterior region be filled with a lossless material. Since both the direct and reflected waves progress entirely within the lossy region, these fields decay exponentially. The lateral wave, on the other hand, proceeds in the exterior lossless environment for most of its trajectory (see for example Fig. 1(b)), and its

dissipative decay is due only to the relatively short path segments in the lossy medium.* This effect is important for the communication between two points located within a bounded lossy material[2], and is relevant as well to propagation within a lossy duct (Fig. 15).[5] The bound waves (surface waves) which may arise in this instance also decay along the entire lateral trajectory within the lossy region.

VI. Reflection and Diffraction of Lateral Waves

The considerations so far have served to describe the behavior of lateral waves excited by sources in regions of quite general composition. The discussion has been limited to single boundaries or interfaces which extend to infinity, thereby assuring the existence of the wave in its pure form. It is, however, relevant to inquire how the lateral wave is modified when the above-mentioned idealized conditions are no longer applicable. We shall consider two types of perturbations which have received detailed attention. The first arises when an additional boundary or interface is inserted, thereby creating a slab or duct region, and the second occurs when the boundary supporting a lateral wave is terminated abruptly. In keeping with the general tenor of this paper, these effects will be discussed in simple physical terms which appeal for their plausibility to the constantly emphasized physical propagation mechanism of the lateral wave. In each instance, a rigorous mathematical justification is available which supports the conclusions reached on purely physical grounds.

A. Lateral Waves in Duct or Slab Regions

When a second boundary is brought into the vicinity of the interface in Fig. 1(b) from the exterior side, a duct of the electrically thinner dielectric is created (Fig. 2(a)). Since the lateral wave field decays exponentially away from the interface in the exterior medium, this second boundary is expected to have little effect as long as

*While it is not possible to define the same ray trajectories in a lossy medium (the dashed ray paths in Fig. 15 are not to be taken literally), the analytical expressions, when continued into the range of complex ϵ, remain valid, thereby justifying these conclusions.

the gap width d is sufficiently large. Detailed analysis substantiates this expectation.[5] For small gap widths, on the other hand, a modification is encountered which may be explained by multiple reflection of the evanescent wave fields.

When a duct is formed by truncating the electrically denser dielectric as in Fig. 15 (see also Fig. 2(b)), the propagating rays refracted back into the medium are reflected and refracted upon reaching the second boundary, thereby giving rise to the multiple trajectories shown by the dots and dashes in Fig. 15. The total lateral wave field at a given observation point is then calculated by summing up the contributions from the various individual lateral waves which arrive via direct, singly reflected, and multiply reflected paths.[5] If the duct is lossy, only the heavily marked trajectory is important since it alone has the smallest path segment in the dissipative region.

B. Reflection of Lateral Waves

A different reflection process is operative when the region is terminated laterally as in Fig. 16(a). One now expects the lateral wave field at an observation point within the denser dielectric to be comprised of two parts: the contribution in the unterminated region plus a reflected contribution as shown in Fig. 16(a) (note the different reflection mechanisms in the two regions separated by the dashed line). The validity of this conjecture is verified by invoking a rigorous image argument which permits replacement of the reflector by an image source (Fig. 16(b)).

C. Excitation of Lateral Waves by Diffraction

Since a source of applied currents in a suitable environment may excite lateral waves, it is not unreasonable to anticipate that sources induced by diffraction give rise to a similar effect. This has been demonstrated on two prototype problems susceptible to rigorous analysis: diffraction by a perfectly conducting half plane in either an isotropic warm plasma[12a] or in an anisotropic cold plasma.[17] As noted in Secs. IIIA and IIIB, either medium, when bounded by a perfectly conducting infinite plane, may support lateral waves which can be excited by an applied line distribution of sources. Since the edge singularity on a half plane acts like a virtual source,

an incident plane wave striking the edge should set up a diffraction field, among the various constituents of which are included the lateral waves. This turns out to be the case[12a], and the resulting ray trajectories for the compressible isotropic plasma, deducible directly from the previous results in Fig. 9, are shown in Fig. 17. ((16) applies as well, with $L_1 = 0$; it is recalled that rays 2 and 3 refer to the optical and acoustic waves, respectively). One finds, furthermore, that the excitation amplitude depends on the equivalent induced source strength at the edge in the same manner as that of the lateral wave in Sec. IIIA depends on the applied source strength, thereby confirming the physical mechanism postulated above. It should be emphasized that these edge-excited lateral waves do not furnish the entire diffraction effect, but that there exist, in addition, radially propagating cylindrical waves as well as surface waves which travel along the screen and decay in the sidewise direction.[12a]

In a similar fashion, one may deduce the lateral waves excited by the edge of the half plane when the latter is embedded in the anisotropic cold plasma described in Sec. IIIB. The trajectories now are those given in Fig. 10(d), with the source located at the edge (i.e., $L_1 = 0$), and the functional dependence is the same as in (17).[17]

D. Diffraction of Lateral Waves

The above-mentioned half plane configuration immersed in the anisotropic cold plasma lends itself to the rigorous demonstration of another interesting effect: diffraction of a lateral wave by the edge discontinuity. If the incident field is generated by a line source and if only the "extraordinary" constituent is considered, one observes from Fig. 10(c) that the incident ray structure is confined to a wedge shaped region about the vertical axis passing through the source. The source may therefore be positioned in such a manner that no direct "e" illumination, confined to the interior of the dashed triangle in Fig. 18, strikes the edge. However, the source excites a lateral wave (see Fig. 10(d), reflected about the vertical axis) which propagates toward the edge and is then diffracted. One expects the diffraction field to include cylindrically spreading waves of the "o" and "e" variety (the "e" field is confined to a

wedge shaped region about the edge), as well as lateral waves reflected from the edge; the latter are shown on the upper side of the half plane, and a similar contribution existing on the lower side has been omitted in order not to complicate the sketch. The trajectories follow at once from Fig. 10(c), and the relevant spatial dependence is deduced from (17), with the amplitude coefficient now determined by the strength of the incident lateral wave field as well as the scattering effect of the edge. These physical concepts are confirmed by the mathematical analysis[17], and it may therefore be concluded that the lateral waves constitute a wave type which may be reflected and diffracted in a manner similar to that encountered among the more familiar geometric-optical wave species. In particular, the validity of the ray picture descriptive of lateral wave propagation, and with it the coupled wave character of the associated wave process, appears amply confirmed by the preceding examples.

VII. Spectral Considerations

It has been demonstrated by the preceding discussion that the lateral wave constitutes a wave species whose well-defined existence depends, however, on the presence of a localized source. The propagation mechanism associated with the lateral wave trajectory is not relevant in the absence of excitation, and one does not therefore expect to encounter this wave constituent in a source-free arrangement. Since source-free solutions satisfying appropriate boundary conditions determine the spectrum of waves which may be guided along a given boundary or interface, it is of interest to inquire into the relation of the lateral waves to the guided wave spectrum.

The simple example of two homogeneous, isotropic dielectrics serves as a relevant illustration. The solution for the field in the denser medium has been given in (1) which constitutes a representation in terms of the continuous mode spectrum along the y-coordinate parallel to the interface (the mode spectrum along y determines the characteristics of the waves guided along z). An alternative representation in terms of the mode spectrum along z (guided waves along y) may be obtained by deformation of the integration contour in Fig. 4(a) about the singularities of the integrand in (1). To this effect, it is convenient to define the multisheeted η surface

in such a manner that the spectral requirement Im $\varkappa_{1,2} > 0$, with $\varkappa_{1,2}$ given in (1a), is satisfied on the entire top sheet. The corresponding branch cuts then follow the rectilinear contours shown in Fig. 19(a) (all of the cuts actually coincide with portions of the real and imaginary axes, but some have been displaced for the sake of clarity). Since no other singularities lie on the top sheet, a deformation of the contour leads to the two branch cut integral contributions in Fig. 19(a). The absence of poles on the "spectral" sheet of the η-surface implies that the spectrum of waves guided along y is wholly continuous.

It may already be surmised from these considerations that the lateral wave has some relation to the continuous spectrum of guided waves along y since its existence was shown to be connected intimately with the branch point at $\eta = k_2$. However, the lateral wave is basically an asymptotic high frequency (or far field) constituent whereas the present discussion concerning the modal representation is unrestricted. To pass on to the high-frequency regime, still another contour integral representation is useful: the steepest descent representation (Fig. 19(b)). The steepest descent path (SDP) is that integration contour along which the integrand decays most rapidly away from the saddle point (see (3)), and its general shape for the present problem is shown in Fig. 19(b).* At high frequencies (or great distance from the source), the principal contributions to the SDP and branch cut integrals arise from the vicinity of the saddle point and branch point, respectively, thereby providing the previously described ray-optical field constituents. The role of the lateral wave may now be characterized more precisely as follows: at observation points lying in its domain of existence, the lateral wave represents compactly the asymptotic contribution from a portion of the continuous spectrum (the portion arising from the k_2-branch point). The remaining (k_1 branch point) portion of the continuous spectrum is

---

*SDP is the complete steepest descent path which ends on the lower Riemann sheet when $k_2 < \eta_s < k_1$; the connection to the endpoints of the original path on the top sheet is then brought about by the branch cut integration P_2. For most applications, the simpler path in Fig. 4(b), which follows the steepest descent contour in the vicinity of the saddle point only, is sufficiently accurate.

represented compactly by the saddle point (geometric-optical) result. Evidently, the asymptotic effect of the continuous spectrum associated with the branch point at k_2 is seen only in certain spatial regions (those reached by the lateral wave), while the spectrum due to the k_1 branch point contributes everywhere.

The characterization of the lateral wave field as a compact representation of the asymptotic contribution of part of the continuous spectrum in special regions of space is reminiscent of another field constituent which behaves in a similar manner: the field contributed by leaky waves. A well-explored prototype structure for the leaky waves is the dielectric gap shown in Fig. 2(a). The field solution in the lower dielectric is given again by the integral in (1) except that the modal reflection coefficient $\Gamma_\infty(\eta)$ for the unbounded upper medium is replaced by $\Gamma(\eta)$ appropriate to the gap configuration.[5] It is found that $\Gamma(\eta)$ retains the branch points at $\pm k_1$, but that a series of complex (leaky wave) poles takes the place of the branch points at $\pm k_2$. These poles do not lie on the spectral Riemann sheet $\text{Im}\, \varkappa_1 \geq 0$, and the spectral representation in terms of waves guided along y, obtained as before by contour deformation (Fig. 20(a)), is therefore again wholly continuous. In the steepest descent representation, the path SDP passes partially into the second Riemann sheet and, for observation points yielding sufficiently large η_s, may intercept there some of the leaky wave poles (Fig. 20(b)). The corresponding residues furnish diffraction contributions to the asymptotic field, in addition to the geometric-optical constituents arising from the saddle point. Since the guided wave spectrum was seen to be continuous, the (improper) leaky wave poles provide a compact asymptotic formulation of a portion of this spectrum in certain spatial regions (i.e., those for which the poles are intercepted by the SDP).

Because of these spectral similarities between the leaky and lateral wave fields, and also from Fig. 2(a) wherein the diffraction field for a gap region is represented in terms of a lateral wave, it is suggestive to seek a quantitative equivalence between these two wave types. Since the decay of a leaky wave along the interface is exponential[18] whereas that of a lateral wave is algebraic, no one-to-one

correspondence is feasible. However, the possibility exists that an accumulation of wave contributions from one species is equivalent to a superposition of those from the other. The validity of this conjecture has been proved for the case of a large gap wherein a ray-optical approach predicts the dominance of a single lateral wave in the diffraction field (Fig. 2(a); the effect of the perfectly conducting boundary is negligible since the lateral wave field is evanescent in the gap). An analysis in terms of leaky waves reveals that the leaky wave poles for the large gap configuration cluster around $\eta = k_2$ and that their cumulative effect may be summed into a closed form descriptive of a single lateral wave field.[5] This establishes a quantitative equivalence which demonstrates furthermore that the ray-optical representation involving a lateral wave is more descriptive of the propagation mechanism in the diffraction field for a large gap than the leaky wave formulation.

VIII. Behavior in Transition Regions

The asymptotic representation of the lateral wave field as in (5), (16) or (17) evidently breaks down when L_k, the lateral path length along the interface, approaches zero. This happens for observation points lying in the vicinity of the angle of total reflection which bounds the region wherein the lateral wave is present (see, for example, the dashed lines in Figs. 1(b) or 10(d)), and the asymptotic procedure in these transition regions must be modified. The analytical feature in the radiation integrals accounting for the transition effect is the presence of a branch point near a saddle point. The required asymptotic technique has been discussed in detail in the literature[2,8] and leads to a parabolic cylinder function as the canonical form characteristic of the field behavior near the boundary of the domain of existence of the lateral wave. The use of this canonical function yields continuous and finite values for the fields as $L_k \to 0$.

IX. Summary

While a general survey of the material contained in this paper has been given in the Introduction, it is not inappropriate to summarize at this time certain salient features. It has been shown that the use of ray optics, combined with the plane wave

refractive index diagrams for the medium (or media) in question, permits the prediction of the types of lateral waves which may be supported on a plane boundary or interface and also leads to the direct construction of the spatial phase and amplitude dependence of the wave.* The media in question can be quite arbitrary, i.e., they may be anisotropic and they may be able to sustain simultaneously electromagnetic and dynamical wave motion. A wave coupling approach has been emphasized which aids in the understanding of the physical propagation mechanism. It has been noted that a rich variety of lateral waves is possible when the composition of the medium is sufficiently general (Figs. 11 and 12).

In the time-harmonic regime which has received primary emphasis in the text, the lateral wave must usually compete with the stronger geometric-optical field, a feature complicating its detection. It is therefore worth emphasizing again that situations do exist where medium inhomogeneity, anisotropy or dissipation renders the lateral wave dominant in certain spatial regions (Sec. V). This aspect should be useful for the independent detection of the wave, either by direct measurement of the field in the region of dominance, or by the introduction into this region of an auxiliary scatterer whose scattered field amplitude is directly proportional to the strength of the impinging lateral wave (some of the considerations in Sec. VI are relevant in this connection). While much experimental evidence on lateral waves is available in the literature on wave propagation in acoustically compressible and elastically deformable media, this is not the case in the electromagnetic regime. Such experimental verification appears highly desirable and may stimulate further interest in the use of the lateral wave as a diagnostic tool or as a carrier of electromagnetic energy.

Some final remarks are in order concerning further analytical work required to provide an understanding of certain lateral wave effects not included in the preceding discussion. One area, that of lateral wave propagation on sharply bounded

---

*A more detailed analysis is required, however, for the evaluation of polarization of the wave and for the dependence of the wave amplitude on the medium parameters.[14]

curved interfaces (Fig. 3), has already been mentioned in the Introduction. A second is concerned with the excitation of lateral waves on "interfaces" between inhomogeneous regions, with the "interface" caused not by a discontinuity in refractive index but by discontinuities in the first or higher derivatives of the index profile. Since the profile itself is continuous, no refraction takes place at the interface, and the lateral wave is excited by the tangent ray. This circumstance may lead to enhanced lateral wave amplitudes[19], and the systematic exploration of the amplitude dependence on the analytical characteristics of the index profile is desirable for the purpose of shedding further light on the propagation mechanism under these conditions. These aspects are presently under consideration at the Electrophysics Department of the Polytechnic Institute of Brooklyn. In addition, further work on transient propagation, especially in dispersive anisotropic regions, would be useful for a clarification of the energy flow characteristics in the lateral waves.

References

1.a. C.B. Officer, "Introduction to the Theory of Sound Transmission", McGraw-Hill Book Company, Inc., New York (1958).

b. W.M. Ewing, W.S. Jardetzky, and F. Press, "Elastic Waves in Layered Media", McGraw-Hill Book Company, Inc., New York (1957).

2. L.M. Brekhovskikh, "Waves in Layered Media", Academic Press, New York (1960). Ch. 4.

3. L.B. Felsen, "On the Use of Refractive Index Diagrams for Source-Excited Anisotropic Regions", Radio Science (NBS), 69D (1965), p.155-169.

4.a. F. Gilbert, "Scattering of Impulsive Elastic Waves by a Smooth Convex Cylinder", J. Acoust. Soc. (Am.), 32 (1960), p. 841-857.

b. Y.M. Chen, "Diffraction by a Smooth Transparent Object", J. Math. Phys., 5 (1964), p. 820-832.

5. T. Tamir and L.B. Felsen, "On Lateral Waves in Slab Configurations and Their Relation to Other Wave Types", IEEE Transactions on Antennas and Propagation, AP-13 (1965), p. 410-422.

6.a. B. van der Pol and A.H.M. Levelt, "On the Propagation of a Discontinuous Electromagnetic Wave", Nederl. Akad. v. Wetenschappen, Amsterdam 63 (1960), p. 254-265.

b. N.J. Vlaar, "The Transient Electromagnetic Field From an Antenna near the Plane Boundary of Two Dielectric Half Spaces", App. Sci. Res. 10B (1963), p. 353-384.

7. D.S. Jones, "The Theory of Electromagnetism", The McMillan Company, New York (1964), Sec. 10.1.

8. L.B. Felsen, "Radiation From a Uniaxially Anisotropic Plasma Half Space", IEEE Transactions on Antennas and Propagation, AP-11 (1963), p. 469-484.

9. L.B. Felsen and B. Rulf, "Radiation from a Directive Antenna Embedded in an Anisotropic Half Space", Electrophysics Department, Polytechnic Institute of Brooklyn, Report PIBMRI-1183-63, August 1963.

10.a K.G. Budden, "Radio Waves in the Ionosphere", Cambridge University Press (1961), Ch. 3.

b. M. Cohen, "Radiation in a Plasma", Phys. Rev., 123 (1961), p. 711-721.

11. A. Hessel, N. Marcuvitz and J. Shmoys, "Scattering and Guided Waves at an Interface Between Air and a Compressible Plasma" IRE Trans. on Antennas and Propagation, AP-10 (1962), p. 48-54.

12.a. F. Labianca and L.B. Felsen, "Diffraction by a Half Plane in a Compressible Plasma", Paper presented at the Symposium on Antennas and Propagation, Washington, D.C., Sept. 30-Aug. 1, 1965

b. S.N. Samaddar, "Electronacoustic Lateral Waves in a Hot Plasma", Raytheon Co., Sudbury, Massachusetts.

13. S. Rosenbaum and L.B. Felsen, "Radiation in Layered Anisotropic Media" Paper presented at URSI Fall Meeting, Dartmouth, New Hampshire, Oct. 1965.

14. L. B. Felsen and S. Rosenbaum, "Ray-Optical Methods for Radiation in Bounded Anisotropic Regions", Electrophysics Dept., Polytechnic Institute of Brooklyn, in preparation.

15. See also G. Tyras, A. Ishimaru and H. M. Swarm, "Lateral Waves in Air-Magnetoplasma Interfaces", Paper in Electromagnetic Theory and Antennas, Pergamon Press, New York (1963), p. 515-535.

16. L. B. Felsen and L. Levey, "A Relation Between a Class of Boundary Value Problems in a Homogeneous and an Inhomogeneous Region", to be published in IEEE Transactions on Antennas and Propagation.

17. S. Rosenbaum and L. B. Felsen, "Diffraction by a Half Plane in an Anisotropic Medium", Electrophysics Dept., Polytechnic Institute of Brooklyn, in preparation.

18. T. Tamir and A. A. Oliner, "Guided Complex Waves, I", Proc. IEE (London), 110 (1963), p. 310-324.

19. Y. Nakamura, "Head Waves from a Linear Transition Layer in a Liquid", J. Geophys. Res., 69 (1964), p. 4349-4354.

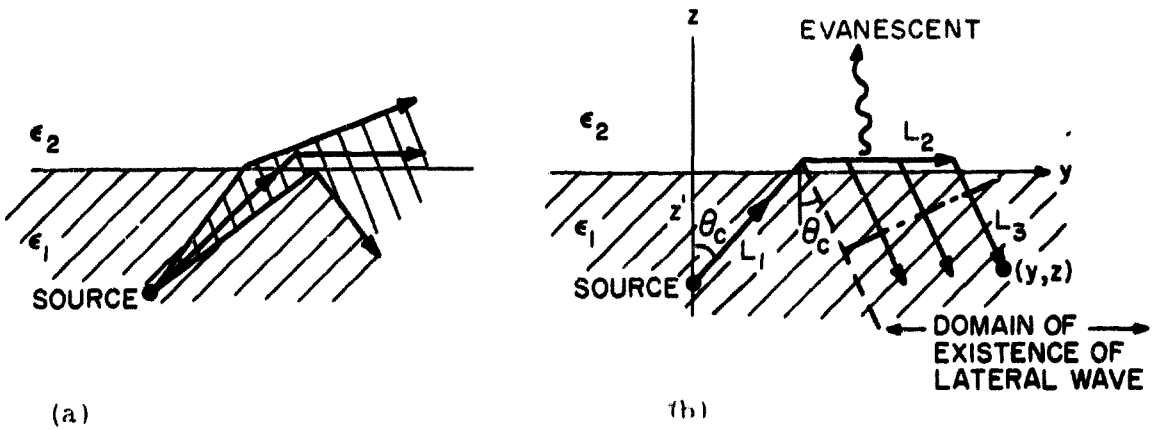

Figure 1 - Ray Considerations (1/2 Section Shown) ($\epsilon_1 > \epsilon_2$)

(a) Ray tube dilemma
(b) Lateral ray trajectory

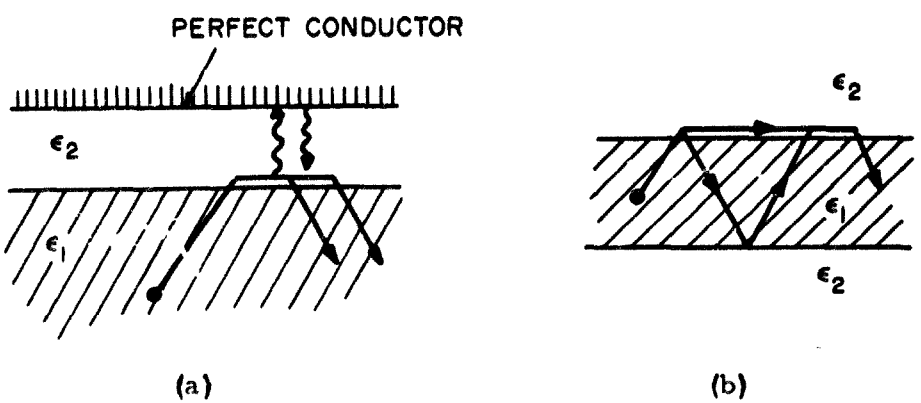

Figure 2 - Lateral Waves in Ducts

(a) Duct in thinner medium
(b) Duct in denser medium

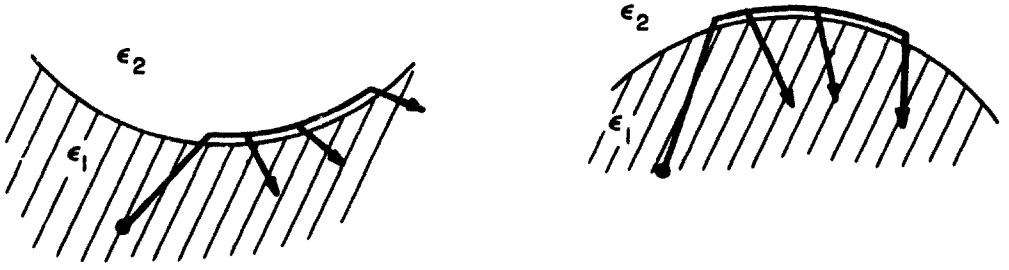

Figure 3 - Lateral Waves on a Curved Boundary

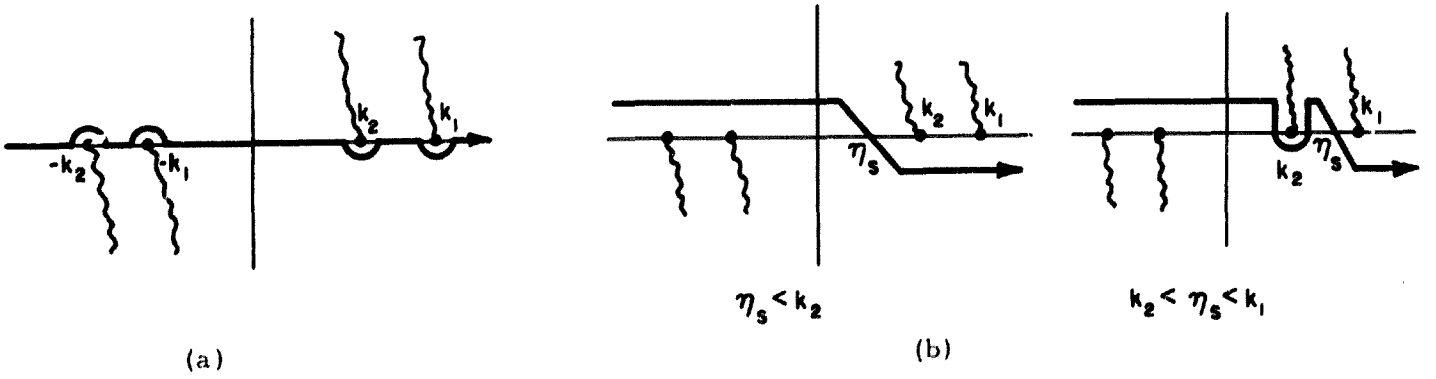

Figure 4 - Integration Paths in Complex η -Plane

(a) Original path
(b) Steepest descent paths

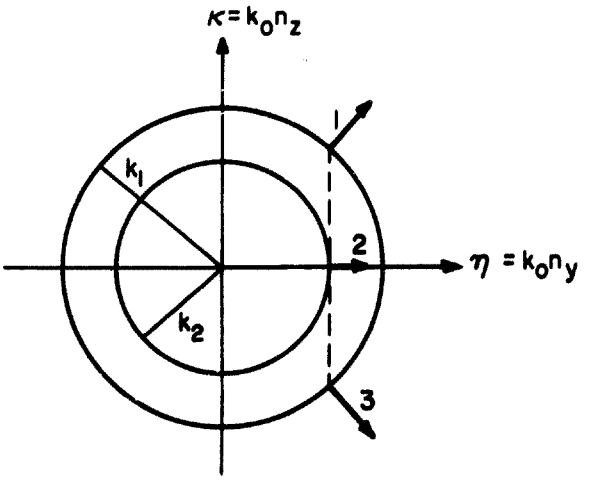

Figure 5 - Wave Number Plot and Rays (Refractive Index = $(1/k_o)$ · wavenumber)

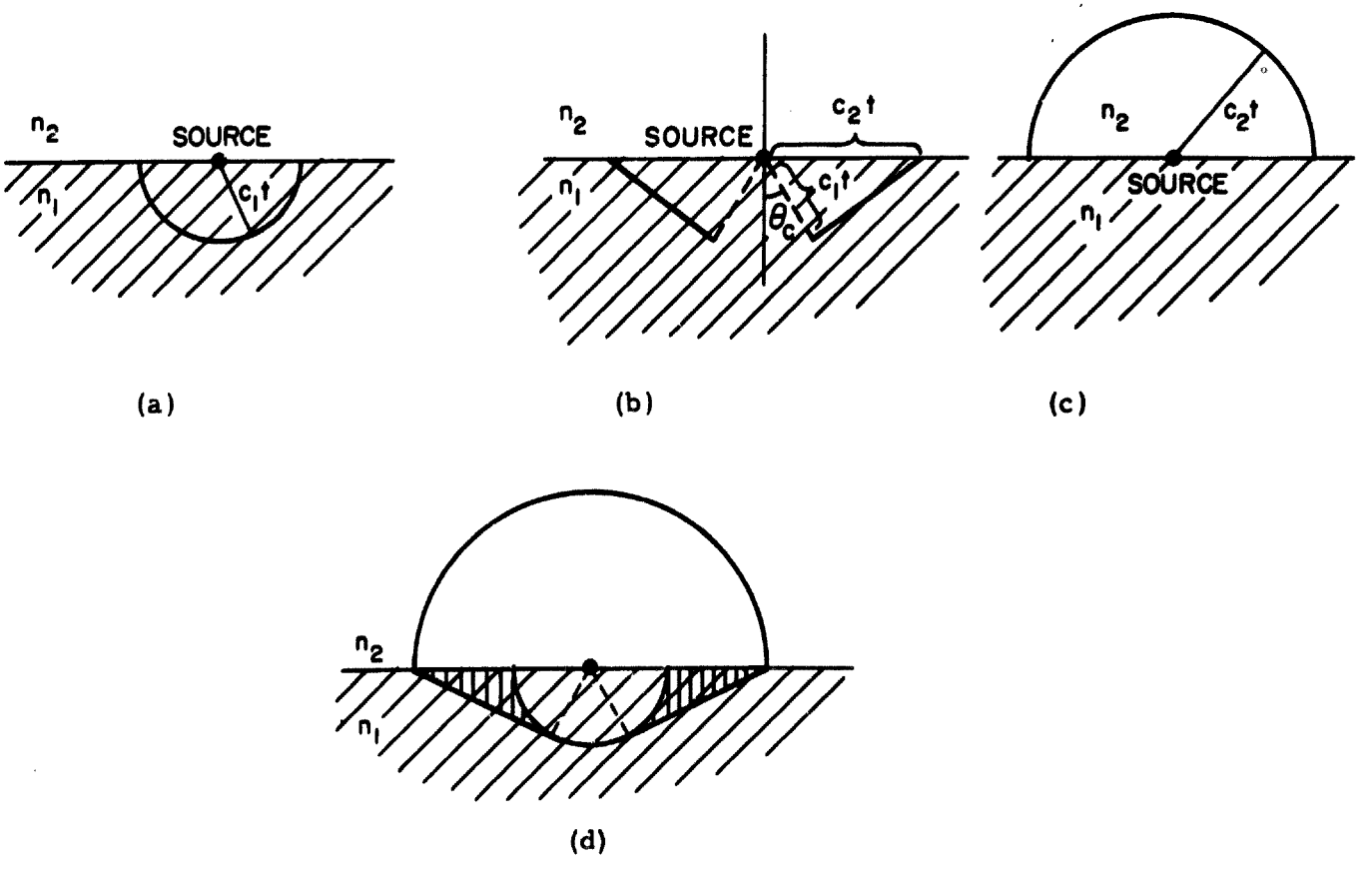

Figure 6 - Various Wave Fronts

(a) Direct - Reflected
(b) Lateral
(c) Refracted
(d) Composite

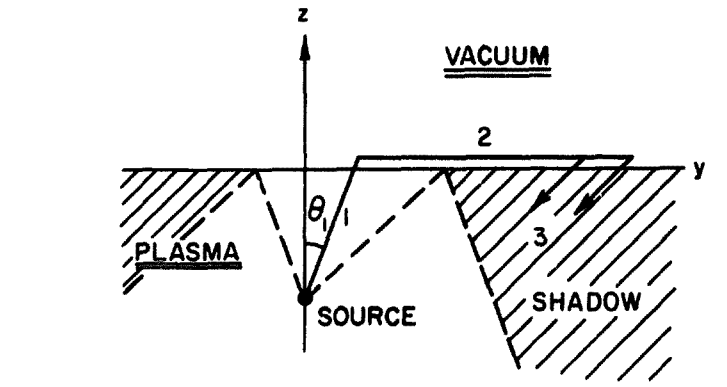

(a)

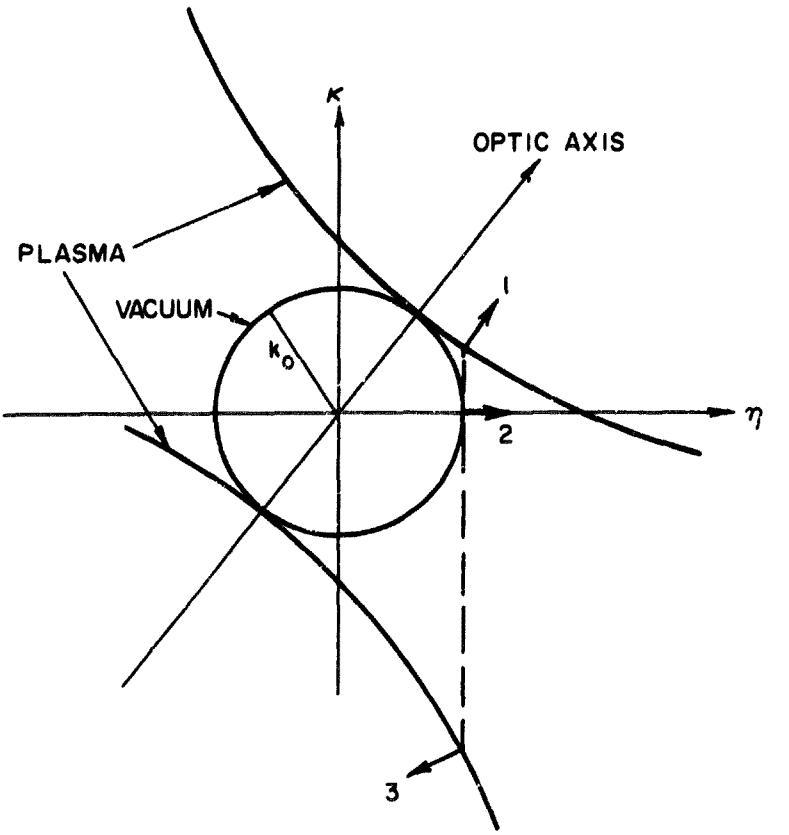

(b)

Figure 7 - Interface Between an Isotropic and a Uniaxially Anisotropic Dielectric

(a) Physical configuration
(b) Wavenumber plot

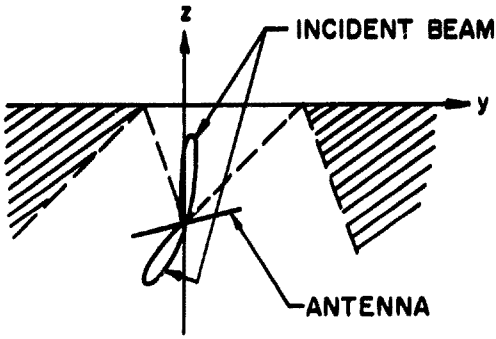

(a)

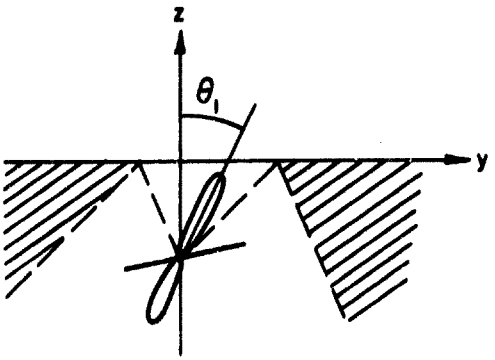

(b)

Figure 8 - Highly Directive Source

(a) Weak excitation of lateral wave
(b) Strong excitation of lateral wave

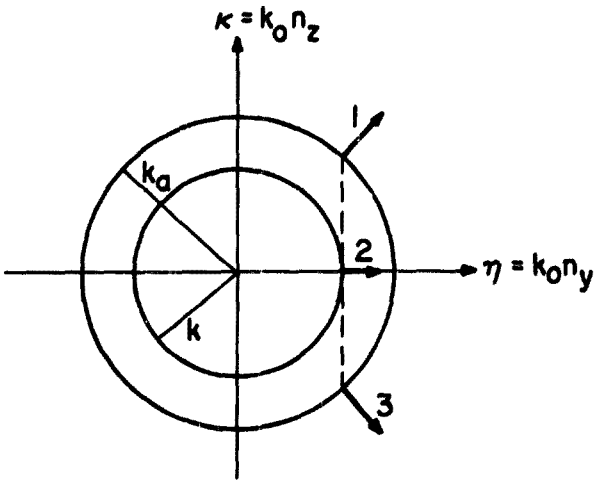

(a)

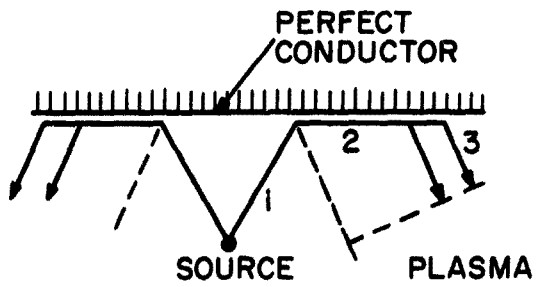

(b)

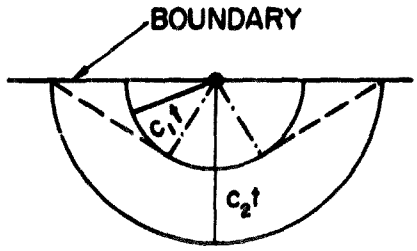

(c)

Figure 9 - Wavenumber Plot and Lateral Wave Trajectory in a Compressible Plasma

(a) Wavenumber plot
(b) Lateral wave trajectory
(c) Wave fronts

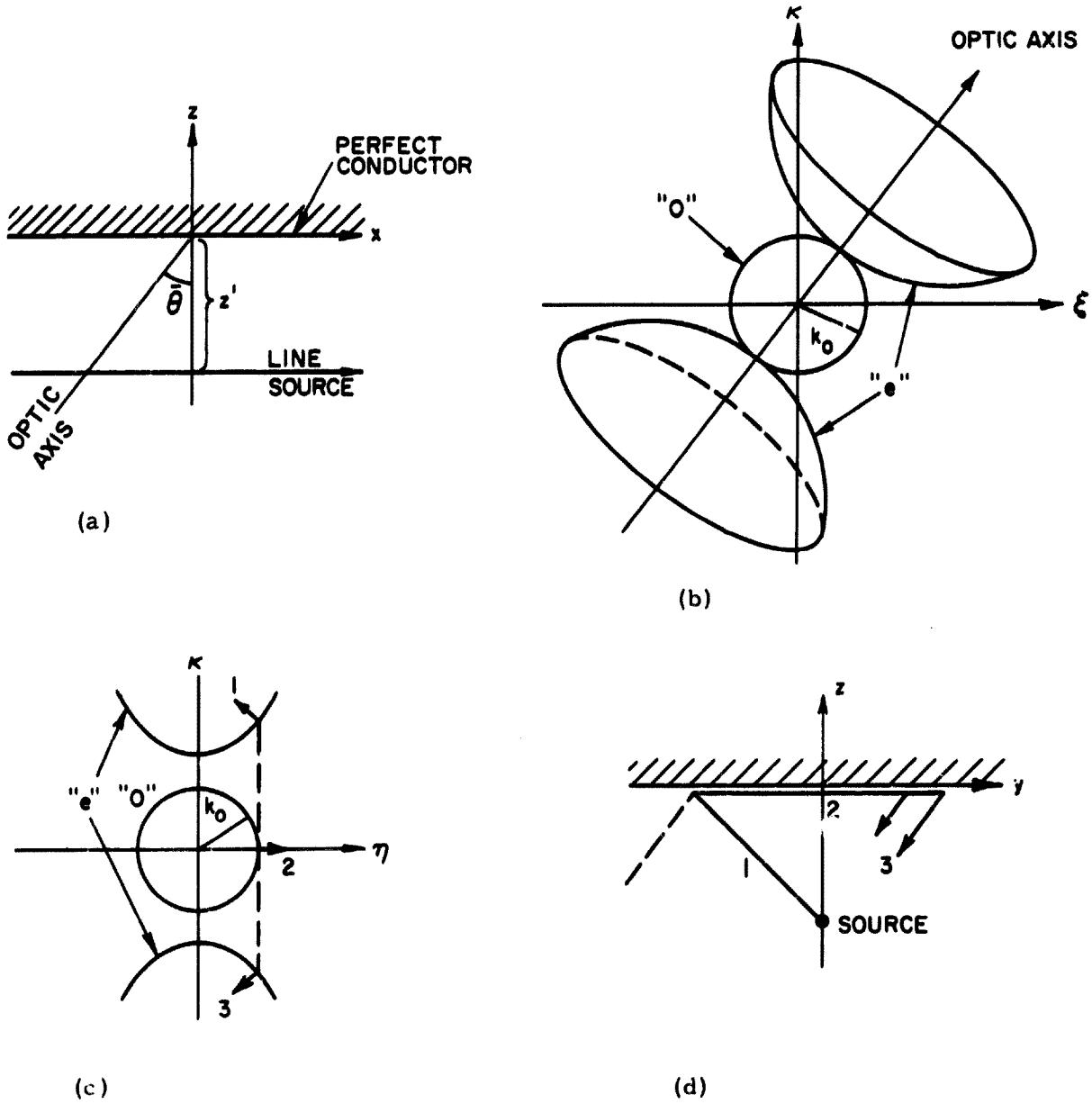

Figure 10 - Uniaxially Anisotropic Medium Excited by Line Source Oblique to Optic Axis

(a) Physical configuration

(b) Wavenumber surface for $\varepsilon < -\tan^2 \bar{\theta}$

(c) Relevant section in κ-η plane

(d) Projection of lateral ray trajectory on y-z plane

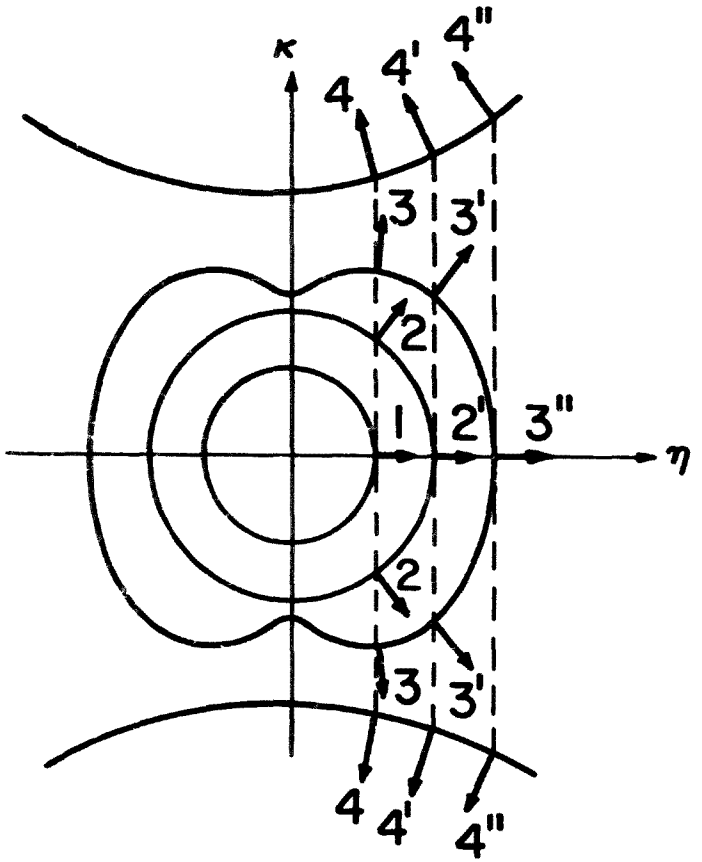

(a)

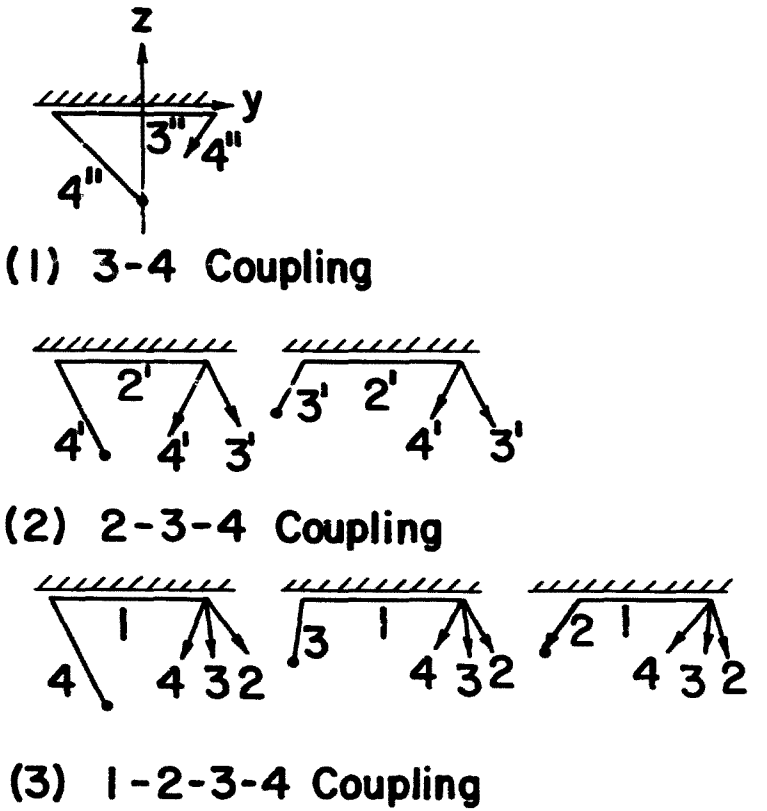

(b)

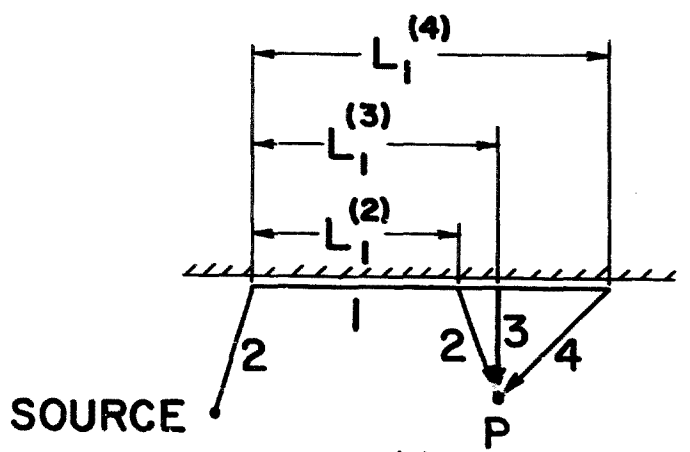

(c)

Figure 11 - Wavenumber surface and lateral ray trajectories for a very general medium

(a) Wavenumber surface
(b) Ray trajectories
(c) Path lengths used for field calculation

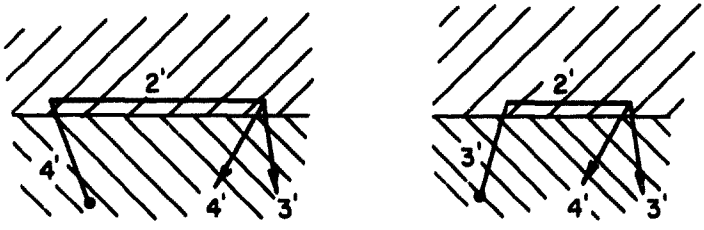

(a)

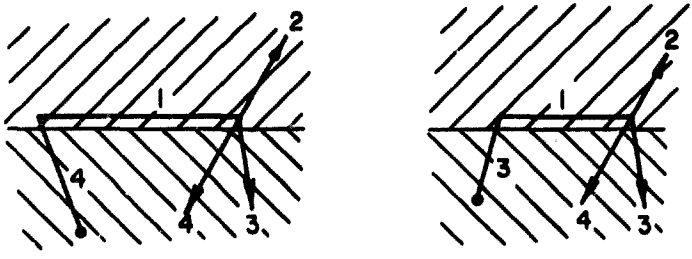

(b)

Figure 12 - Lateral ray Trajectories for Two-Medium Problem, Each Having Two Wave Species

(a) 2-3-4 coupling
(b) 1-2-3-4 coupling

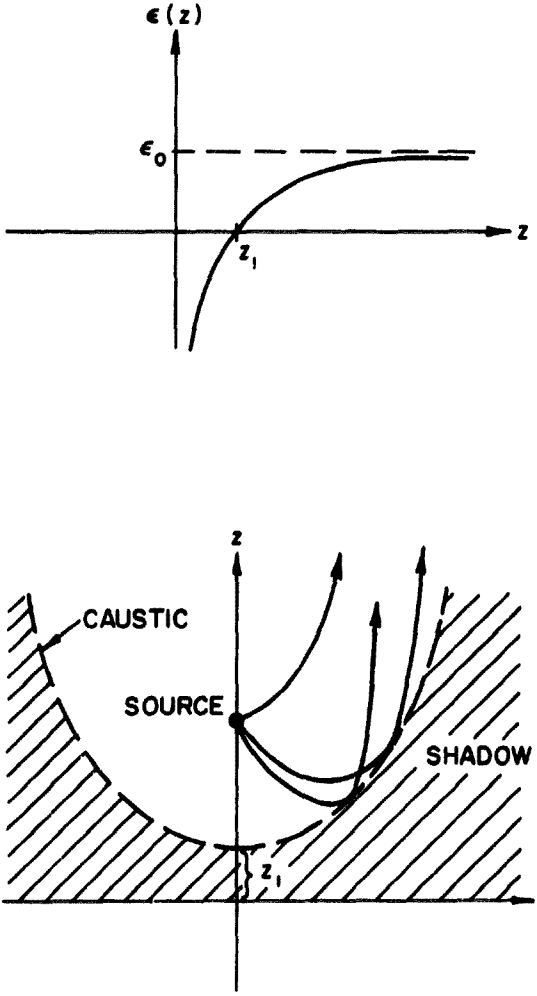

Figure 13 - Rays in an Unbounded Inhomogeneous Isotropic Medium

(a) Profile
(b) Geometric-Optical ray structure

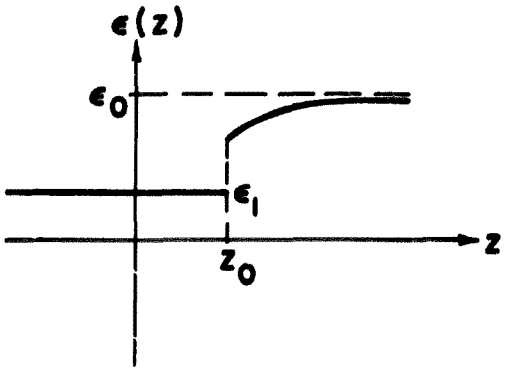

(a)

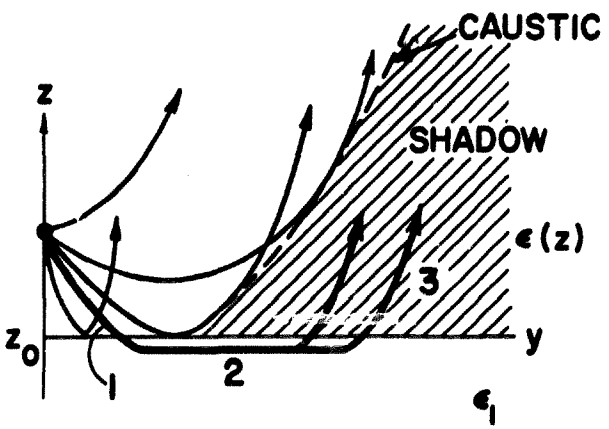

(b)

Figure 14 - Rays in Composite Region

(a) Profile
(b) Ray structure (lateral ray drawn heavy)

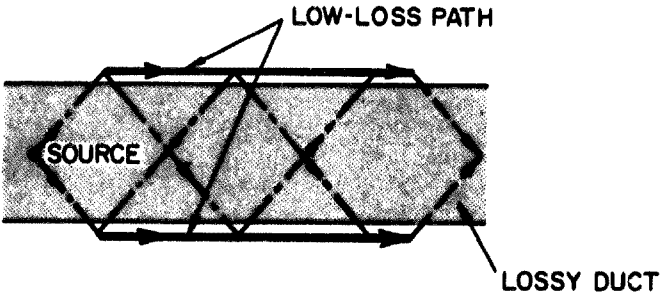

Figure 15 - Propagation in a Lossy Duct

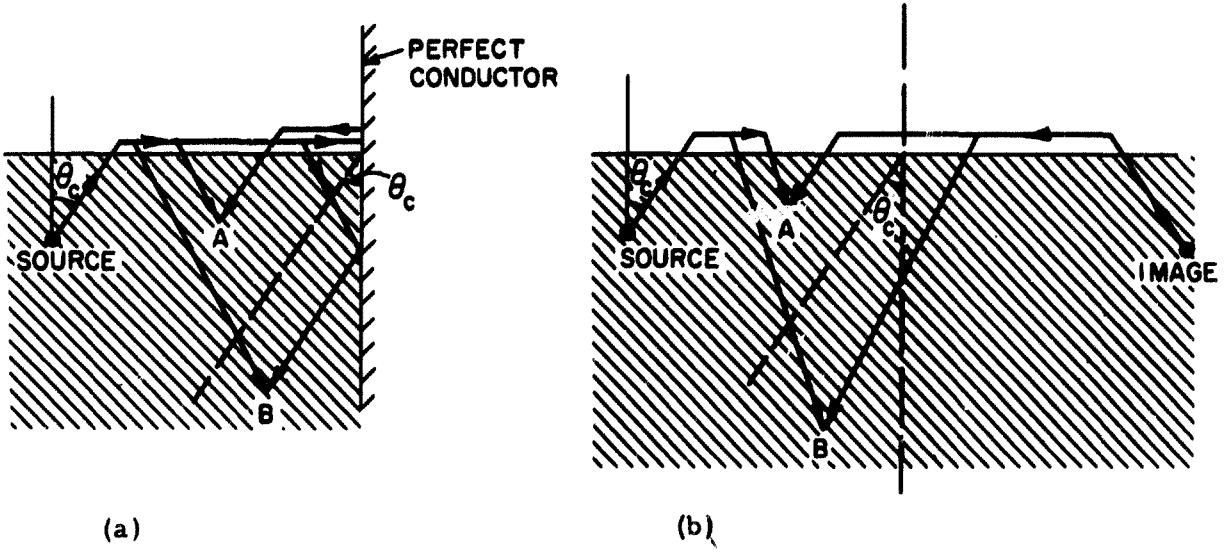

Figure 16 - Reflection by a Lateral Termination

(a) Actual configuration
(b) Equivalent configuration

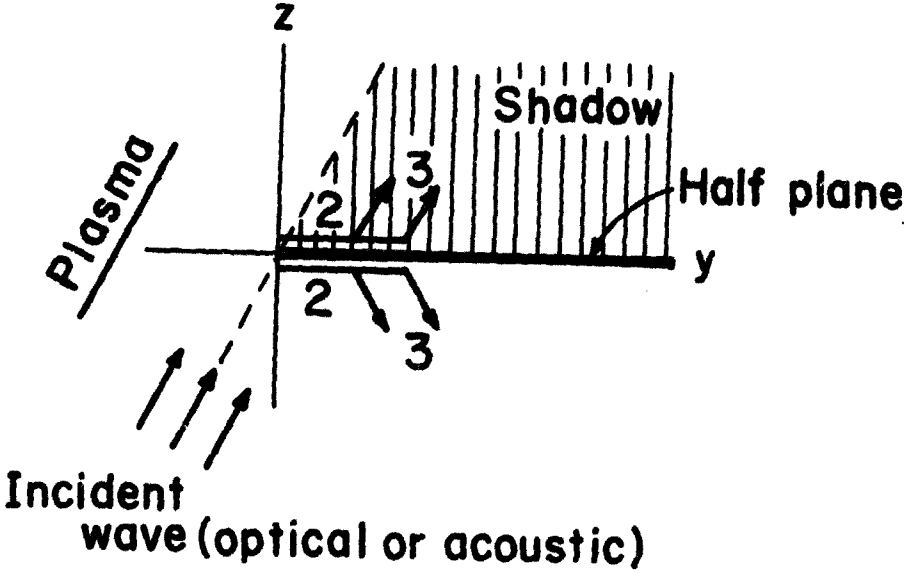

Figure 17 - Lateral Waves Excited by Diffraction in a Compressible Isotropic Plasma

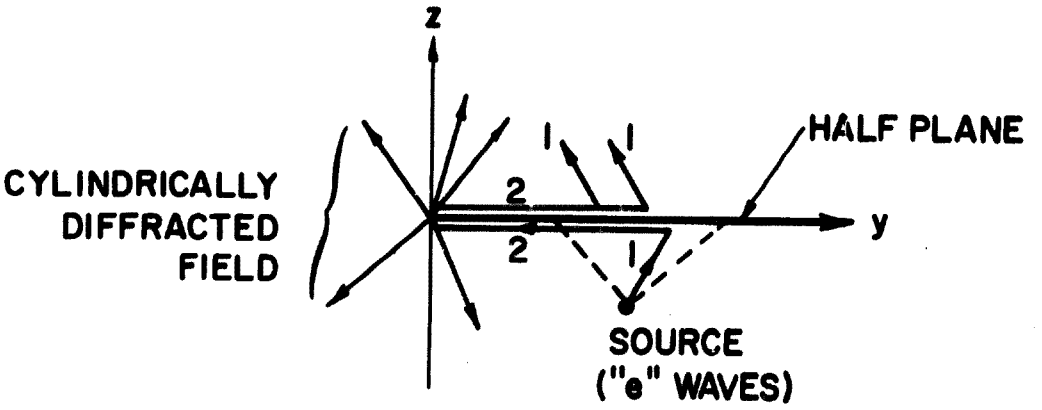

Figure 18 - Diffraction of a Lateral Wave by an Edge

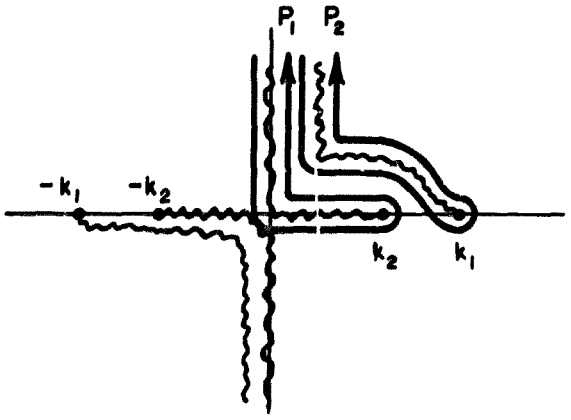

(a)

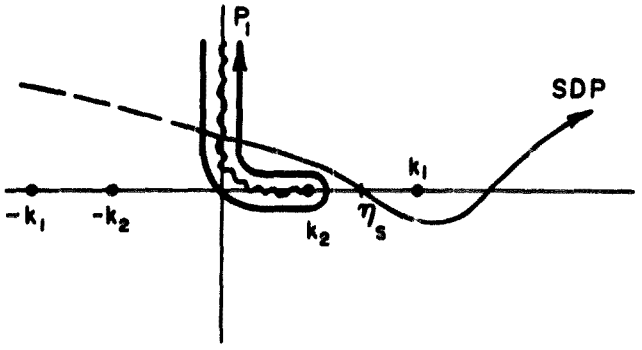

(b)

Figure 19 - Various Integration Contours in the Complex η -Plane for the Problem Involving Two Adjoining Half Spaces

(a) Contours for Guided Wave Representation along y
(b) Contours for steepest descent Representation

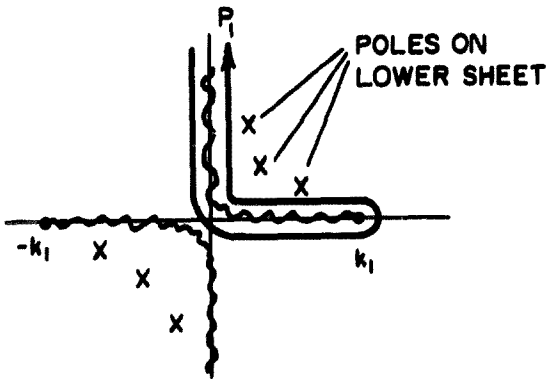

(a)

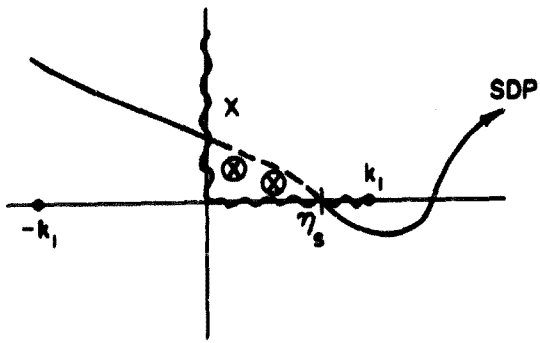

(b)

Figure 20 - Various Integration Paths in the Complex η -Plane for the Gap Problem

(a) Contour for guided wave representation along y

(b) Contours for steepest descent representation

Unclassified

Security Classification

DOCUMENT CONTROL DATA - R&D

(Security classification of title, body of abstract and indexing annotation must be entered when the overall report is classified)

1. ORIGINATING ACTIVITY (Corporate author) Polytechnic Institute of Brooklyn, Graduate Center Route 110, Farmingdale, New York 11735	2a. REPORT SECURITY CLASSIFICATION Unclassified 2b. GROUP

3. REPORT TITLE

LATERAL WAVES

4. DESCRIPTIVE NOTES (Type of report and inclusive dates)

Research Report

5. AUTHOR(S) (Last name, first name, initial)

Felsen, Leopold B.

6. REPORT DATE	7a. TOTAL NO. OF PAGES	7b. NO. OF REFS
15 November 1965	53	19

8a. CONTRACT OR GRANT NO.	9a. ORIGINATOR'S REPORT NUMBER(S)
AF 19(628)-2357 b. PROJECT NO. and Task 5635, 01	PIBMRI-1303-65
c. DOD element 61445014 d. DOD subelement 681305	9b. OTHER REPORT NO(S) (Any other numbers that may be assigned this report) AFCRL-65-889

10. AVAILABILITY/LIMITATION NOTICES Qualified requestors may obtain copies of this report from DDC. Other persons or organizations should apply to the Clearinghouse for Federal Scientific and Technical Information (CFSTI), Sills Building, 5285 Port Royal Road, Springfield, Virginia 22151

11. SUPPLEMENTARY NOTES	12. SPONSORING MILITARY ACTIVITY
	Hq. AFCRL, OAR (CRD) US Air Force, L.G. Hanscom Field Bedford, Massachusetts

13. ABSTRACT When a radiator is located in a region wherein two or more wave types (1,2,..) may propagate with different speeds, and when a boundary coupling these wave types is present, diffraction phenomena may arise which are describable in terms of lateral waves. A lateral wave is launched by that portion of the incident field of type 1, for example, which gives rise to a field of type 2 refracted parallel to the boundary and which in turn refracts into a field of type 1. The most familiar example involves a plane interface separating two different semi-infinite dielectrics, and the associated wave types are the incident-reflected and the refracted waves. However, in anisotropic or in mechanically deformable media which may support several wave species, lateral waves are excited even in the absence of a second region.

The properties of lateral waves are reviewed in the transient and in the time-harmonic regimes. Concepts of wave coupling are emphasized, and general analytical features, as well as graphical procedures using refractive index diagrams, are described. Illustrative examples exhibit lateral waves on the interface between two homogeneous or inhomogeneous dielectrics, on a perfectly conducting plane immersed in an anisotropic and (or) compressible plasma, and also on a perfectly conducting half plane. The latter example shows how lateral waves may be diffracted by an edge discontinuity. Some relations between lateral waves, leaky waves, and spectral representations are also included.

DD FORM 1 JAN 64 1473

Unclassified

Security Classification

14. KEY WORDS	LINK A		LINK B		LINK C	
	ROLE	WT	ROLE	WT	ROLE	WT
Lateral waves Wave coupling Anisotropic plasmas Warm plasmas Interface effects						

INSTRUCTIONS

1. ORIGINATING ACTIVITY: Enter the name and address of the contractor, subcontractor, grantee, Department of Defense activity or other organization *(corporate author)* issuing the report.

2*a*. REPORT SECURITY CLASSIFICATION: Enter the overall security classification of the report. Indicate whether "Restricted Data" is included. Marking is to be in accordance with appropriate security regulations.

2*b*. GROUP: Automatic downgrading is specified in DoD Directive 5200.10 and Armed Forces Industrial Manual. Enter the group number. Also, when applicable, show that optional markings have been used for Group 3 and Group 4 as authorized.

3. REPORT TITLE: Enter the complete report title in all capital letters. Titles in all cases should be unclassified. If a meaningful title cannot be selected without classification, show title classification in all capitals in parenthesis immediately following the title.

4. DESCRIPTIVE NOTES: If appropriate, enter the type of report, e.g., interim, progress, summary, annual, or final. Give the inclusive dates when a specific reporting period is covered.

5. AUTHOR(S): Enter the name(s) of author(s) as shown on or in the report. Enter last name, first name, middle initial. If military, show rank and branch of service. The name of the principal author is an absolute minimum requirement.

6. REPORT DATE: Enter the date of the report as day, month, year; or month, year. If more than one date appears on the report, use date of publication.

7*a*. TOTAL NUMBER OF PAGES: The total page count should follow normal pagination procedures, i.e., enter the number of pages containing information.

7*b*. NUMBER OF REFERENCES: Enter the total number of references cited in the report.

8*a*. CONTRACT OR GRANT NUMBER: If appropriate, enter the applicable number of the contract or grant under which the report was written.

8*b*, 8*c*, & 8*d*. PROJECT NUMBER: Enter the appropriate military department identification, such as project number, subproject number, system numbers, task number, etc.

9*a*. ORIGINATOR'S REPORT NUMBER(S): Enter the official report number by which the document will be identified and controlled by the originating activity. This number must be unique to this report.

9*b*. OTHER REPORT NUMBER(S): If the report has been assigned any other report numbers *(either by the originator or by the sponsor)*, also enter this number(s).

10. AVAILABILITY/LIMITATION NOTICES: Enter any limitations on further dissemination of the report, other than those imposed by security classification, using standard statements such as:

(1) "Qualified requesters may obtain copies of this report from DDC."

(2) "Foreign announcement and dissemination of this report by DDC is not authorized."

(3) "U. S. Government agencies may obtain copies of this report directly from DDC. Other qualified DDC users shall request through _____."

(4) "U. S. military agencies may obtain copies of this report directly from DDC. Other qualified users shall request through _____."

(5) "All distribution of this report is controlled. Qualified DDC users shall request through _____."

If the report has been furnished to the Office of Technical Services, Department of Commerce, for sale to the public, indicate this fact and enter the price, if known.

11. SUPPLEMENTARY NOTES: Use for additional explanatory notes.

12. SPONSORING MILITARY ACTIVITY: Enter the name of the departmental project office or laboratory sponsoring *(paying for)* the research and development. Include address.

13. ABSTRACT: Enter an abstract giving a brief and factual summary of the document indicative of the report, even though it may also appear elsewhere in the body of the technical report. If additional space is required, a continuation sheet shall be attached.

It is highly desirable that the abstract of classified reports be unclassified. Each paragraph of the abstract shall end with an indication of the military security classification of the information in the paragraph, represented as *(TS), (S), (C), or (U)*.

There is no limitation on the length of the abstract. However, the suggested length is from 150 to 225 words.

14. KEY WORDS: Key words are technically meaningful terms or short phrases that characterize a report and may be used as index entries for cataloging the report. Key words must be selected so that no security classification is required. Identifiers, such as equipment model designation, trade name, military project code name, geographic location, may be used as key words but will be followed by an indication of technical context. The assignment of links, rules, and weights is optional.

GPO 886-551